JHEP

Published for SISSA by Springer

Received: May 4, 2016
Revised: August 12, 2016
Accepted: September 24, 2016
Published: October 10, 2016

Ward identity and Homes' law in a holographic superconductor with momentum relaxation

Kyung Kiu Kim,[a,b] **Miok Park**[c] **and Keun-Young Kim**[a]

[a] *School of Physics and Chemistry, Gwangju Institute of Science and Technology, 123 Cheomdan-gwagiro, Gwangju 61005, Korea*

[b] *Department of Physics, College of Science, Yonsei University, 50 Yonsei-ro, Seoul 120-749, Korea*

[c] *School of Physics, Korea Institute for Advanced Study, 85 Hoegiro, Seoul 130-722, Korea*

E-mail: kimkyungkiu@gmail.com, miokpark76@gmail.com, fortoe@gist.ac.kr

Abstract: We study three properties of a holographic superconductor related to conductivities, where momentum relaxation plays an important role. First, we find that there are constraints between electric, thermoelectric and thermal conductivities. The constraints are analytically derived by the Ward identities regarding diffeomorphism from field theory perspective. We confirm them by numerically computing all two-point functions from holographic perspective. Second, we investigate Homes' law and Uemura's law for various high-temperature and conventional superconductors. They are empirical and (material independent) universal relations between the superfluid density at zero temperature, the transition temperature, and the electric DC conductivity right above the transition temperature. In our model, it turns out that the Homes' law does not hold but the Uemura's law holds at small momentum relaxation related to coherent metal regime. Third, we explicitly show that the DC electric conductivity is finite for a neutral scalar instability while it is infinite for a complex scalar instability. This shows that the neutral scalar instability has nothing to do with superconductivity as expected.

Keywords: Holography and condensed matter physics (AdS/CMT), Gauge-gravity correspondence

ArXiv ePrint: 1604.06205

doi:10.1007/JHEP10(2016)041

JHEP10(2016)041

Contents

1 Introduction **1**

2 AC conductivities: holographic model and method **4**
- 2.1 Equilibrium state 4
- 2.2 AC conductivities 6

3 Conductivities with a neutral scalar hair instabitliy **9**
- 3.1 Charged scalar case ($q \neq 0$) 9
- 3.2 Neutral scalar case ($q = 0$) 10
- 3.3 General expression for superfluid density 12

4 Ward identities: constraints between conductivities **14**
- 4.1 Analytic derivation: field theory 15
- 4.2 Numerical confirmation: holography 19
- 4.3 Conductivities at small ω 20

5 Homes' law and Uemura's law **22**

6 Conclusion and discussions **26**

A Two-point functions related to the real scalar operator **27**

JHEP10(2016)041

1 Introduction

Holographic methods have provided novel and effective tools to study strongly correlated systems [1–6] and they have been applied to many condensed matter problems. In particular, holographic understanding of high T_c superconductor is one of the important issues. The first holographic superconductor model was proposed by Hartnoll, Herzog, and Horowitz (HHH)[1] [7, 8], and there have been extensive development of the model. For reviews and references, we refer to [2, 3, 9, 10].

The HHH model is a translationally invariant system with finite charge density. Therefore, it cannot relax momentum and exhibits an infinite electric DC conductivity even in normal phase not only in superconducting phase. To construct more realistic superconductor models, some methods incorporating momentum relaxation were proposed. One way of including momentum relaxation is to break translational invariance explicitly by imposing inhomogeneous (spatially modulated) boundary conditions on a bulk field [11–15]. Massive gravity models [16–22] give some gravitons mass terms, which breaks bulk diffeomorphism and translation invariance in the boundary field theory. Holographic Q-lattice

[1]The HHH model is a class of Einstein-Maxwell-complex scalar action with negative cosmological constant. It is based on the action (2.1) with $\psi_I = 0$. The holographic interpretation of this model is reviewed in section 2.

models [23–27] take advantage of a global symmetry of the bulk theory. For example, a global phase of a complex scalar plays a role of breaking translational invariance. Models with massless scalar fields linear in spatial coordinate [28–38] utilize the shift symmetry. Some models with a Bianchi VII_0 symmetry are dual to helical lattices [39–41]. Based on these models, holographic superconductor incorporating momentum relaxation have been developed [42–51].

In this paper, we study the HHH holographic superconductor model with massless scalar fields linear in spatial coordinate [46], where the strength of momentum relaxation is identified with the proportionality constant to spatial coordinate. The property of the normal phase of this model such as thermodynamics and transport coefficients were studied in [28, 30–32, 52–54]. The superconducting phase was analysed in [45, 46]. In particular, optical electric, thermoelectric and thermal conductivities of the model have been extensively studied in [31, 46, 53, 54]. Building on them, we further investigate interesting properties related to conductivities and momentum relaxation. There are three issues that we want to address in this paper: (1) conductivities with a neutral scalar hair instability, (2) Ward identities: constraints between conductivities, (3) Homes' law and Uemura's law. We explain each issue in the following.

(1) In a holographic superconductor model of a Einstein-Maxwell-scalar action [8, 9], a superconducting state is due to the formation of a complex scalar field, Φ, with the charge q in a bulk spacetime below a critical temperature. It amounts to breaking U(1) symmetry spontaneously by an expectation value of the charged operator. The formation of the scalar hair Φ may be understood as the coupling of the charged scalar to the charge of the black hole through the covariant derivative $D_M\Phi \equiv \nabla_M\Phi - iqA_M\Phi$, which gives an effective mass of Φ as $m^2_{\text{eff}} \equiv m^2 - q^2|g^{tt}|A_t^2$. m^2_{eff} may be sufficiently negative near the horizon to destabilize the scalar field. Based on this argument one may expect that when $q = 0$ the instability would turn off. However, it turns out that a Reissner-Nordstrom AdS black hole may still be unstable to forming *neutral* scalar hair. This instability is not associated with superconductivity because it does not break a U(1) symmetry, but at most breaks a $\mathbb{Z}_2$ symmetry $\Phi \to -\Phi$. Therefore, in this system with a neutral scalar hair, it is natural to expect that DC electric conductivity will be finite contrary to the case with a complex scalar hair (superconductor). However, to our knowledge, this argument has not been explicitly checked yet. In the HHH models without momentum relaxation, this question is not well posed since electric conductivity is always infinite due to translation invariance. In this paper, in a model with momentum relaxation, we show that DC electric conductivity that derived from the neutral hairy black hole is indeed finite.

(2) Three transport coefficients, electric conductivity(σ), thermoelectric conductivity(α) and thermal conductivity($\bar{\kappa}$), are identified by the retarded two-point functions of two operators, electric current(J) and heat current(Q). See (4.55) for explicit expressions. It was shown, in normal phase without momentum relaxation, there are two constraints relating three transport coefficients, σ, α, and $\bar{\kappa}$ [3, 55]. The constraints can be derived by the Ward identities regarding diffeomorphism and U(1) gauge symmetry. In our model, there is an extra bulk field, a massless scalar intro-

JHEP10(2016)041

duced for momentum relaxation. Therefore, we have another scalar operator, say S, in the dual field theory and consequently we have six two-point functions of three operators, J, Q, and S. It turns out, in this case, there are three Ward identities of six two-point functions: σ, α and $\bar{\kappa}$ and three two-point functions related to the operator S. If $S = 0$, thanks to the two constraints, α and $\bar{\kappa}$ can be obtained algebraically once σ is computed numerically. This is why only σ is presented in the literature [2]. However, if $S \neq 0$, the information of σ alone cannot determine α and $\bar{\kappa}$, which must be computed independently. In this paper, following the method in [3], we first derive the Ward identities for two-point functions analytically from field theory perspective. Next, we confirm them numerically by computing all two functions by holographic methods. This confirmation of the Ward identities also demonstrates the faithfulness of our numerical method.

(3) Homes' law and Uemura's law are empirical and material independent universal laws for high-temperature and some conventional superconductors [56, 57]. The law states that, for various superconductors, there is a *universal* material independent relation between the superfluid density ($\tilde{\rho}_s$) at near zero temperature and the transition temperature ($\tilde{T}_c$) multiplied by the electric DC conductivity ($\sigma_{\rm DC}$) in the normal state right above the transition temperature $\tilde{T}_c$.

$$\tilde{\rho}_s(\tilde{T} = 0) = C\sigma_{\rm DC}(\tilde{T}_c)\,\tilde{T}_c\,, \tag{1.1}$$

where $\tilde{\rho}_s$, $\tilde{T}_c$ and $\sigma_{\rm DC}$ are scaled to be dimensionless, and C is a dimensionless universal constant: $C \approx 4.4$ or 8.1. They are computed in [47] from the experimental data in [56, 57]. For in-plane high T_c superconductors and clean BCS superconductors $C \approx 4.4$. For c-axis high T_c superconductors and BCS superconductors in the dirty limit $C \approx 8.1$. Notice that momentum relaxation is essential here because without momentum relaxation $\sigma_{\rm DC}$ is infinite. There is another similar universal relation, Uemura's law, which holds only for underdoped cuprates [56, 57]:

$$\tilde{\rho}_s(\tilde{T} = 0) = B\,\tilde{T}_c\,, \tag{1.2}$$

where B is another universal constant. In the context of holography Homes' law was studied in [47, 58]. It was motivated [58] by holographic bound of the ratio of shear viscosity to entropy density (η/s) in strongly correlated plasma [1] and its understanding in terms of quantum criticality [59] or Planckian dissipation [60],where the time scale of dissipation is shortest possible. Since Homes' law also may arise in systems of Planckian dissipation [60] there is a good chance to find universal physics in condensed matter system as well as in quark-gluon plasma. In [47] Homes' law was observed in a holographic superconductor model in a helical lattice for some restricted parameter regime of momentum relaxation, while Uemura's law did not hold in that model. However, physic behind Homes' law in this model has not been clearly understood yet. For further understanding on Homes' law, in this paper, we have checked Homes' law and Uemuras' law in our holographic superconductor model. We find that Homes' law does not hold but Uemura's law holds at small momentum relaxation region, related to coherent metal regime.

JHEP10(2016)041

This paper is organised as follows. In section 2, we introduce our holographic superconductor model incorporating momentum relaxation by massless real scalar fields. The equilibrium state solutions and the method to compute AC conductivities are briefly reviewed. In section 3, the conductivities with a neutral scalar instability are computed and compared with the ones with a complex hair instability. In section 4, we first derived Ward identities giving constraints between conductivities analytically from field theory perspective. These identities are confirmed numerically by holographic method. In section 5, after analysing conductivities at small frequency, we discuss the Home's law and Uemura's law in our model. In section 6 we conclude.

2 AC conductivities: holographic model and method

2.1 Equilibrium state

In this section we briefly review the holographic superconductor model we study, referring to [28, 31, 53, 54, 61] for more complete and detailed analysis. We consider the action[2]

$$S = \int \mathrm{d}^4x\sqrt{-g}\left[R - 2\Lambda - \frac{1}{4}F^2 - |D\Phi|^2 - m^2|\Phi|^2 - \frac{1}{2}\sum_{I=1}^{2}(\partial\psi_I)^2\right], \tag{2.1}$$

where $x^M = \{t, x, y, r\}$ and r is the holographic direction. R is the Ricci scalar and $\Lambda = -3/L^2$ is the cosmological constant with the AdS radius $L = 1$. We have included the field strength $F = \mathrm{d}A$ for a U(1) gauge field A, the complex scalar field Φ with mass m, two massless scalar fields, $\psi_I (I = 1, 2)$. The covariant derivative is defined by $D_M\Phi \equiv \nabla_M\Phi - iqA_M\Phi$ with the charge q of the complex scalar field. However, if $q = 0$, Φ is a neutral scalar not a charged scalar. We consider a neutral scalar and a charged scalar in section 3, where it will be shown that a neutral scalar case does not correspond to superconductors. Having this observation we consider only a charged scalar in section 4 and 5, because we are investigating properties of superconductors in those sections.

The action (2.1) yields equations of motion

$$R_{MN} - \frac{1}{2}g_{MN}\left(R + 6 - \frac{1}{4}F^2 - |D\Phi|^2 - m^2|\Phi|^2 - \frac{1}{2}\sum_{I=1}^{2}(\partial\psi_I)^2\right)$$
$$= \frac{1}{2}F_{MQ}F_N{}^Q + \frac{1}{2}\left(D_M\Phi D_N\Phi^* + D_N\Phi D_M\Phi^*\right) + \frac{1}{2}\sum_{I=1}^{2}\partial_M\psi_I\partial_N\psi_I\,, \tag{2.2}$$

$$\nabla_M F^{MN} = -iq(\Phi^* D^N\Phi - \Phi D^N\Phi^*)\,, \tag{2.3}$$

$$\left(D^2 - m^2\right)\Phi = 0\,, \qquad \nabla^2\psi_I = 0\,, \tag{2.4}$$

for which we make the following ansatz:

$$A = A_t(r)\mathrm{d}t + \frac{1}{2}B\,(x\mathrm{d}y - y\mathrm{d}x)\,, \qquad \Phi = \Phi(r)\,, \quad \psi_I = (\beta x, \beta y)\,, \tag{2.5}$$

$$\mathrm{d}s^2 = -\mathrm{U}(r)e^{-\chi(r)}\mathrm{d}t^2 + \frac{\mathrm{d}r^2}{\mathrm{U}(r)} + r^2(\mathrm{d}x^2 + \mathrm{d}y^2)\,. \tag{2.6}$$

[2]The complete action includes also the Gibbons Hawking term and some boundary terms for holographic renormalization, which are explained in [28, 31, 53, 54, 61] in more detail.

JHEP10(2016)041

Via the holographic dictionary, $A_t(r)$ encodes a finite chemical potential or charge density and B plays a role of an external magnetic field. $\Phi(r)$ is dual to a superconducting phase order parameter, condensate. Near boundary ($r \to \infty$), $\Phi \sim \frac{J^\Phi}{r^{3-\Delta}} + \frac{\langle \mathcal{O}^\Phi \rangle}{r^\Delta} + \dots$ with two undetermined coefficients J^Φ and $\langle \mathcal{O}^\Phi \rangle$, which are identified with the source and condensate respectively. The dimension Δ of the condensate is related to the bulk mass of the complex scalar by $m^2 = \Delta(\Delta - 3)$. In this paper, we take $m^2 = -2$ and $\Delta = 2$ to perform numerical analysis. ψ_I is introduced to give momentum relaxation effect where β is the parameter for the strength of momentum relaxation. For $\beta = 0$, the model becomes the original holographic superconductor proposed by Hartnoll, Herzog, and Horowitz (HHH) [7, 8].

One way to understand momentum relaxation effect by ψ_I is to see the Ward identity related to the boundary stress tensor of the model (2.1) when $\Phi = 0$ [28]:

$$\nabla_\nu \langle T^{\nu\mu} \rangle = -F_\nu{}^\mu \langle J^\nu \rangle - \nabla^\mu \psi_I \langle O_I \rangle \,, \tag{2.7}$$

where μ, ν are indices in the field theory $x^\mu = (t, x, y)$. If we consider a homogeneous and isotopic system in flat spacetime the left hand side becomes the time derivative of the momentum (say $\mu = x$),

$$\langle \dot{P}^x \rangle = E^x \langle J^t \rangle - \partial^x \psi_I \langle O^I \rangle \,, \tag{2.8}$$

where $\langle P^x \rangle \equiv \langle T^{tx} \rangle$, $E^x \equiv F^{tx}$ and assume a finite density system without current, i.e. $J^\nu = (J^t, 0, 0)$. The first term on the right hand side is a driving force, which is the boundary electric field (E^x) times the charge density (J^t). The second term plays a role of friction and gives momentum relaxation. By choosing $\psi_I = (\beta x, \beta y)$ with constant β as in (2.5) we can achieve nonzero dissipation in a homogeneous and isotropic system.

First, if $\Phi(r) = 0$ (no condensate), the solution corresponds to a normal state and its analytic formula is given by

$$\begin{aligned} \mathrm{U}(r) &= r^2 - \frac{\beta^2}{2} - \frac{m_0}{r} + \frac{n^2 + B^2}{4r^2} \,, \qquad \chi(r) = 0, \\ A_t &= n \left(\frac{1}{r_h} - \frac{1}{r} \right) \,, \end{aligned} \tag{2.9}$$

where r_h is the location of the black brane horizon defined by $\mathrm{U}(r_h) = 0$, $m_0 \equiv r_h^3 - \frac{\beta^2 r_h}{2} + \frac{n^2+B^2}{4r_h}$, and n is interpreted as charge density. It is the dyonic black brane [62] modified by β due to ψ_I [54]. The thermodynamics and transport coefficients(electric, thermoelectric, and thermal conductivity) of this system was analysed in detail in [54]. In the case without magnetic field, see [31]. Next, if $\Phi(r) \neq 0$, the solution corresponds to a superconducting state with finite condensate and its analytic formula is not available.[3] For $B = 0$, the solutions are numerically obtained in [8] for $\beta = 0$ and in [46] for $\beta \neq 0$. For example we display numerical solutions for some cases in figure 1, where we set $r_h = 1$ and plot dimensionless quantities scaled by μ: $\mathrm{U}(r)/\mu^2$, A_t/μ, and χ. For $B \neq 0$, due to the generation of vortex our ansatz (2.5) should be modified. In this paper we will not consider this case and refer to [2, 63, 64].

[3] A nonzero $\Phi(r)$ induces a nonzero $\chi(r)$, which changes the definition of 'time' at the boundary so field theory quantities should be defined accordingly.

JHEP10(2016)041

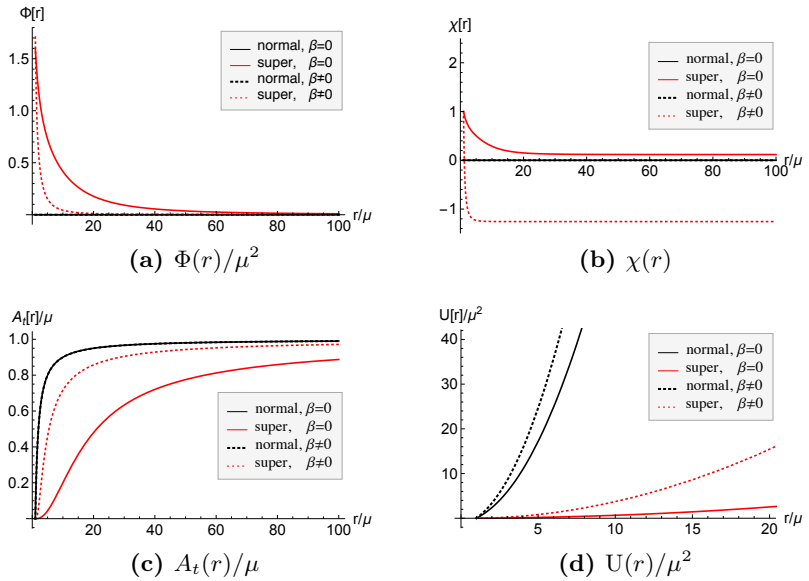

(a) $\Phi(r)/\mu^2$ **(b)** $\chi(r)$

(c) $A_t(r)/\mu$ **(d)** $\mathrm{U}(r)/\mu^2$

Figure 1. Numerical solutions of bulk background functions, which are numerically integrated from the black hole horizon ($r_h = 1$). The solid curves are for the case without momentum relaxation ($\beta = 0$) while the dotted curves are for momentum relaxation ($\beta/\mu = 0.5$). The black curves are for normal phase ($\langle \mathcal{O}^\Phi \rangle = 0$) while the red curves are for superconducting phase ($\langle \mathcal{O}^\Phi \rangle \neq 0$). In (a), (b) and (c) the black solid and dotted curves are coincide, but in (d) they are different. The black curves agree to the analytic formula in (2.9), where β enters only into $\mathrm{U}(r)$.

2.2 AC conductivities

The purpose of this subsection is to briefly describe the essential points of a method to compute the AC thermo-electric conductivities. For more details and clarification regarding our model at $B = 0$, see [53, 54] for normal phase and [46] for superconducting phase. At $B \neq 0$ see [31] for normal phase.

In order to study transport phenomena holographically, we introduce small bulk fluctuations around the background obtained in the previous subsection. For example, to compute electric, thermoelectric, and thermal conductivities it is enough to consider

$$\begin{aligned} \delta A_i(t,r) &= \int_{-\infty}^{\infty} \frac{\mathrm{d}\omega}{2\pi} e^{-i\omega t} a_i(\omega, r)\,, \\ \delta g_{ti}(t,r) &= \int_{-\infty}^{\infty} \frac{\mathrm{d}\omega}{2\pi} e^{-i\omega t} r^2 h_{ti}(\omega, r)\,, \\ \delta \psi_i(t,r) &= \int_{-\infty}^{\infty} \frac{\mathrm{d}\omega}{2\pi} e^{-i\omega t} \xi_i(\omega, r)\,, \end{aligned} \tag{2.10}$$

where $i = x, y$ for $B \neq 0$ and $i = x$ is enough for $B = 0$ thanks to a rotational symmetry in $x - y$ space. For the sake of illustration of our method, we consider the case for $B = 0$ [46] and refer to [54] for $B \neq 0$. In momentum space, the linearized equations of motion around

JHEP10(2016)041

the background are[4]

$$\begin{aligned} a_x'' + \left(\frac{U'}{U} - \frac{\chi'}{2}\right) a_x' + \left(\frac{\omega^2}{U^2} e^{\chi} - \frac{2q^2\Phi^2}{U}\right) a_x + \frac{r^2 e^{\chi} A_t'}{U} h_{tx}' = 0\,, \\ h_{tx}' + \frac{A_t'}{r^2} a_x + \frac{i\beta U e^{-\chi}}{r^2\omega} \xi' = 0\,, \\ \xi_x'' + \left(\frac{U'}{U} - \frac{\chi'}{2} + \frac{2}{r}\right) \xi_x' - \frac{i\beta\omega e^{\chi}}{U^2} h_{tx} + \frac{\omega^2 e^{\chi}}{U^2} \xi_x = 0\,. \end{aligned} \tag{2.11}$$

Near boundary ($r \to \infty$) the asymptotic solutions are

$$\begin{aligned} h_{tx} &= h_{tx}^{(0)} + \frac{1}{r^2} h_{tx}^{(2)} + \frac{1}{r^3} h_{tx}^{(3)} + \cdots\,, \\ a_x &= a_x^{(0)} + \frac{1}{r} a_x^{(1)} + \cdots\,, \\ \xi_x &= \xi_x^{(0)} + \frac{1}{r^2} \xi_x^{(2)} + \frac{1}{r^3} \xi_x^{(3)} + \cdots\,. \end{aligned} \tag{2.12}$$

The on-shell quadratic action in momentum space reads

$$S_{\text{ren}}^{(2)} = \frac{1}{2} \int \frac{\mathrm{d}\omega}{2\pi} \left[J_{-\omega}^a \mathbb{A}_{ab}(\omega) J_{\omega}^b + J_{-\omega}^a \mathbb{B}_{ab}(\omega) R_{\omega}^b \right], \tag{2.13}$$

where

$$J^a = \begin{pmatrix} a_x^{(0)} \\ h_{tx}^{(0)} \\ \xi_x^{(0)} \end{pmatrix}, \quad R^a = \begin{pmatrix} a_x^{(1)} \\ h_{tx}^{(3)} \\ \xi_x^{(3)} \end{pmatrix}, \quad \mathbb{A} = \begin{pmatrix} 0 & -n & 0 \\ 0 & 2U^{(1)} & 0 \\ 0 & 0 & 0 \end{pmatrix}, \quad \mathbb{B} = \begin{pmatrix} 1 & 0 & 0 \\ 0 & -3 & 0 \\ 0 & 0 & 3 \end{pmatrix}. \tag{2.14}$$

Here $U^{(1)}$ is the coefficient of $1/r$ when $\mathrm{U}(r)$ is expanded near boundary and n is charge density. The index ω in J^a and R^a are suppressed.

The remaining task for reading off the retarded Green's function is to express R^b in terms of J^a. It can be done by the following procedure. First let us denote small fluctuations in momentum space by Φ^a collectively. i.e.

$$\Phi^a = (\delta a_i\,, \delta h_{ti}\,, \delta\xi_i)\,. \tag{2.15}$$

Near black brane horizon ($r = 1$), solutions may be expanded as

$$\Phi^a(r) = (r-1)^{-\frac{i\omega}{4\pi T} + n^a} \left(\varphi^a + \tilde{\varphi}^a (r-1) + \cdots\right), \tag{2.16}$$

which corresponds to incoming boundary conditions for the retarded Green's function [65] and n^a is some integer depending on specific fields, Φ^a. The leading terms φ^a are only free parameters and the higher order coefficients such as $\tilde{\varphi}^a$ are determined by the equations

[4]For $B \neq 0$ case, the bulk fluctuations to y direction should be turned on so the number of equations of motion are doubled too.

JHEP10(2016)041

of motion. A general choice of φ^a can be written as a linear combination of independent basis φ_i^a, $(i = 1, 2, \cdots, N)$, i.e. $\varphi^a = \sum_{i=1}^N \varphi_i^a c_i$. For example, φ_i^a can be chosen as

$$\begin{pmatrix} \varphi_1^a & \varphi_2^a & \dots & \varphi_N^a \end{pmatrix} = \begin{pmatrix} 1 & 1 & \dots & 1 \\ 1 & -1 & \dots & 1 \\ \vdots & \vdots & \ddots & \vdots \\ 1 & 1 & \dots & -1 \end{pmatrix} . \tag{2.17}$$

Every φ_i^a yields a solution $\Phi_i^a(r)$, which is expanded near boundary as

$$\Phi_i^a(r) \to \mathbb{S}_i^a + \cdots + \frac{\mathbb{O}_i^a}{r^{\delta_a}} + \cdots , \tag{2.18}$$

where $\delta_a \geq 1$ and the leading terms $\mathbb{S}_i^a$ are the *sources* of i-th solutions and $\mathbb{O}_i^a$ are the corresponding *operator* expectation values. $\mathbb{S}$ and $\mathbb{O}$ can be regarded as regular matrices of order N, where a is for row index and i is for column index. A general solution may be constructed from a basis solution set $\{\Phi_i^a\}$:

$$\Phi^a(r) = \Phi_i^a(r) c^i \to \mathbb{S}_i^a c^i + \cdots + \frac{\mathbb{O}_i^a c^i}{r^{\delta_a}} + \cdots \tag{2.19}$$

$$\equiv J^a + \cdots + \frac{R^a}{r^{\delta_a}} + \cdots , \tag{2.20}$$

with arbitrary constants c^i's. For a given J^a, we always can find c^i,[5]

$$c^i = (\mathbb{S}^{-1})_a^i J^a , \tag{2.21}$$

so the corresponding response R^a may be expressed in terms of the sources J^b,

$$R^a = \mathbb{O}_i^a c^i = \mathbb{O}_i^a (\mathbb{S}^{-1})_b^i J^b . \tag{2.22}$$

With (2.22), the action (2.13) becomes

$$\begin{aligned} S_{\text{ren}}^{(2)} &= \frac{1}{2} \int_{\omega \geq 0} \frac{\mathrm{d}\omega}{2\pi} \left[J_{-\omega}^a \left[\mathbb{A}_{ab}(\omega) + \mathbb{B}_{ac} \mathbb{O}_i^c (\mathbb{S}^{-1})_b^i(\omega) \right] J_\omega^b \right] \\ &\equiv \frac{1}{2} \int_{\omega \geq 0} \frac{\mathrm{d}\omega}{2\pi} \left[J_{-\omega}^a G_{ab} J_\omega^b \right] , \end{aligned} \tag{2.23}$$

where the range of ω is chosen to be positive following the prescription in [65] and the retarded Green's functions are explicitly denoted as

$$G_{ab} \equiv \begin{pmatrix} G_{JJ} & G_{JT} & G_{JS} \\ G_{TJ} & G_{TT} & G_{TS} \\ G_{SJ} & G_{ST} & G_{SS} \end{pmatrix} . \tag{2.24}$$

[5] There is one subtlety in our procedure. The matrix $\mathbb{S}$ of solutions with incoming boundary condition are not invertible and we need to add some constant solutions, which is related to a residual gauge fixing $\delta g_{rx} = 0$ [53].

JHEP10(2016)041

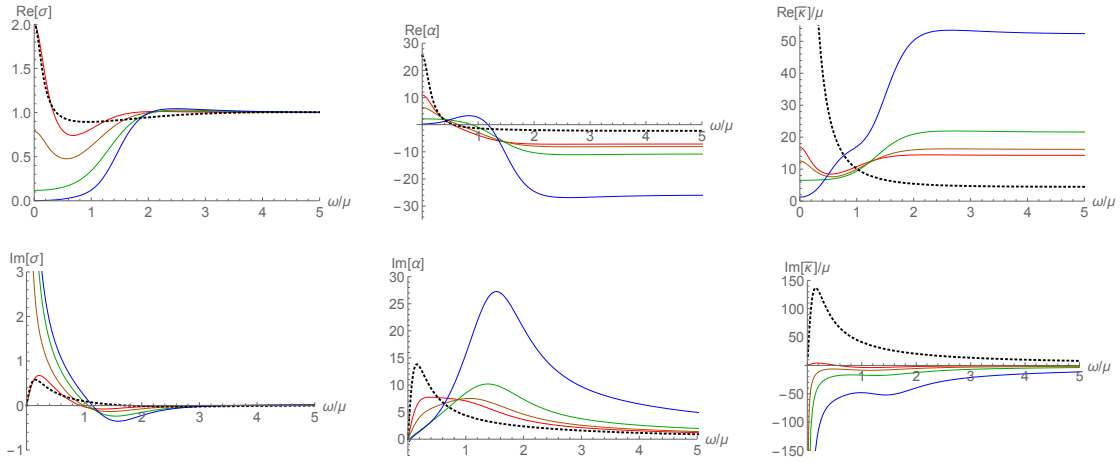

(a) Electric conductivity **(b)** Thermoelectric conductivity **(c)** Thermal conductivity

Figure 2. AC electric conductivity($\sigma(\omega)$), thermoelectric conductivity($\alpha(\omega)$), and thermal conductivity($\bar{\kappa}(\omega)$) for $\beta/\mu = 1$ and $q = 3$ at different temperatures: $T/T_c = 3.2, 1, 0.89, 0.66, 0.27$ (dotted, red, orange,green, blue). Top is the real part and bottom is the imaginary part of conductivities.

Finally, the thermo-electric conductivities are related to the retarded Green's functions as

$$\begin{pmatrix} \sigma & \alpha T \\ \bar{\alpha} T & \bar{\kappa} T \end{pmatrix} = -\frac{i}{\omega} \begin{pmatrix} G_{JJ} & -\mu G_{JJ} + G_{JT} \\ -\mu G_{JJ} + G_{TJ} & G_{TT} - G_{TT}(\omega = 0) - \mu \left(G_{JT} + G_{TJ} - \mu G_{JJ} \right) \end{pmatrix}. \tag{2.25}$$

3 Conductivities with a neutral scalar hair instabitliy

In this section we present our numerical results of the electric, thermoelectric and thermal conductivities of the model (2.1), which are obtained by the numerical method reviewed in the previous subsection. There are two cases: i) with a charged scalar hair ($q \neq 0$) or ii) with a neutral scalar hair ($q = 0$), where q is defined below (2.1) through the covariant derivative $D_M \Phi \equiv \nabla_M \Phi - iqA_M \Phi$.

3.1 Charged scalar case ($q \neq 0$)

The first case with $q \neq 0$ have been computed in [31, 46, 54]. As an example, in figure 2, we show the results for $B = 0, q = 3$ [46], which is reproduced here for easy comparison with new results in this paper. Figure 2 shows AC electric conductivity ($\sigma(\omega)$), thermoelectric conductivity ($\alpha(\omega)$), and thermal conductivity ($\bar{\kappa}(\omega)$) for $\beta/\mu = 1$ and $q = 3$ at different temperatures. The colors of curves represent the temperature ratio, T/T_c, where T_c is the critical temperature of metal/superconductor phase transition. $T/T_c = 3.2, 1, 0.89, 0.66, 0.27$ for dotted, red, orange,green, and blue curves respectively. In particular, the dotted curve is the case above T_c and the red curve corresponds to the

JHEP10(2016)041

critical temperature. The first row is the real part and the second row is the imaginary part of conductivities.

One feature we want to focus on in figure 2 is $1/\omega$ pole in $\mathrm{Im}[\sigma]$ below the critical temperature. There is no $1/\omega$ pole above the critical temperature. By the Kramers-Kronig relation, the $1/\omega$ pole in $\mathrm{Im}[\sigma]$ implies the existence of the delta function at $\omega = 0$ in $\mathrm{Re}[\sigma]$. It means that in superconducting phase the DC conductivity is infinite while in normal phase the DC conductivity is finite due to momentum relaxation.

3.2 Neutral scalar case ($q = 0$)

Unlike the studies in [46], here we set $q = 0$ (a neutral scalar hair). Between finite q and zero q, there is a qualitative difference in the instability of a Reissner-Nordstrom AdS black hole [8]. The origin of the superconductor (or superfluidity) instability responsible for the complex scalar hair Φ may be understood as the coupling of the charged scalar to the charge of the black hole through the covariant derivative $D_M\Phi \equiv \nabla_M\Phi - iqA_M\Phi$. In other words, the effective mass of Φ defined by $m^2_{\text{eff}} \equiv m^2 - q^2|g^{tt}|A_t^2$ can be compared with the Breitenlohner-Freedman (BF) bound. The BF bound for AdS_{d+1} is $-\frac{d^2}{4} \equiv m^2_{\text{BF}}$. The effective mass m^2_{eff} may be sufficiently negative near the horizon to destabilize the scalar field since $|g^{tt}|$ becomes bigger at low temperature.[6] Based on this argument one may expect that when $q = 0$ the instability would turn off. However, it turns out that a Reissner-Nordstrom AdS black hole may still be unstable to forming *neutral* scalar hair, if m^2 is a little bit bigger than the BF bound for AdS_4. It can be understood by the near horizon geometry of an extremal Reissner-Nordstrom AdS black hole. It is $\mathrm{AdS}_2\times \mathrm{R}^2$ so scalars above the BF bound for AdS_4 may be below the bound for AdS_2. These two instability conditions can be summarized by one inequality [46]

$$m^2_{\text{eff}} = \left[m^2 - \frac{2q^2}{1+\frac{\beta^2}{\mu^2}}\right]\left[\frac{1}{6}\left(1+\frac{\frac{\beta^2}{\mu^2}}{1+\frac{\beta^2}{\mu^2}}\right)\right] < -\frac{1}{4} = m^2_{\text{BF}}\,, \tag{3.1}$$

which reproduces the result for $\beta = 0$ in [2]:

$$m^2_{\text{eff}} = \left(m^2 - 2q^2\right)\left(\frac{1}{6}\right) < -\frac{1}{4} = m^2_{\text{BF}}\,. \tag{3.2}$$

Here, we see m^2_{eff} can be below the BF bound when $q = 0$.

However, it was discussed in [8, 9] that the instability to forming neutral scalar hair for $q = 0$ is not associated with superconductivity because it does not break a U(1) symmetry, but at most breaks a $\mathbb{Z}_2$ symmetry $\Phi \to -\Phi$. Therefore, it would be interesting to see if the DC conductivity is infinite or not in the background with a neutral scalar hair.[7] Without momentum relaxation ($\beta = 0$) this question is not well posed since the DC conductivity is always infinite with or without a neutral scalar hair due to translation invariance and finite density. Now we have a model with momentum relaxation ($\beta \neq 0$), we can address this issue properly.

[6] As the temperature of a charged black hole is decreased, g_{tt} develops a double zero at the horizon.

[7] We thank Sang-Jin Sin for suggesting this.

JHEP10(2016)041

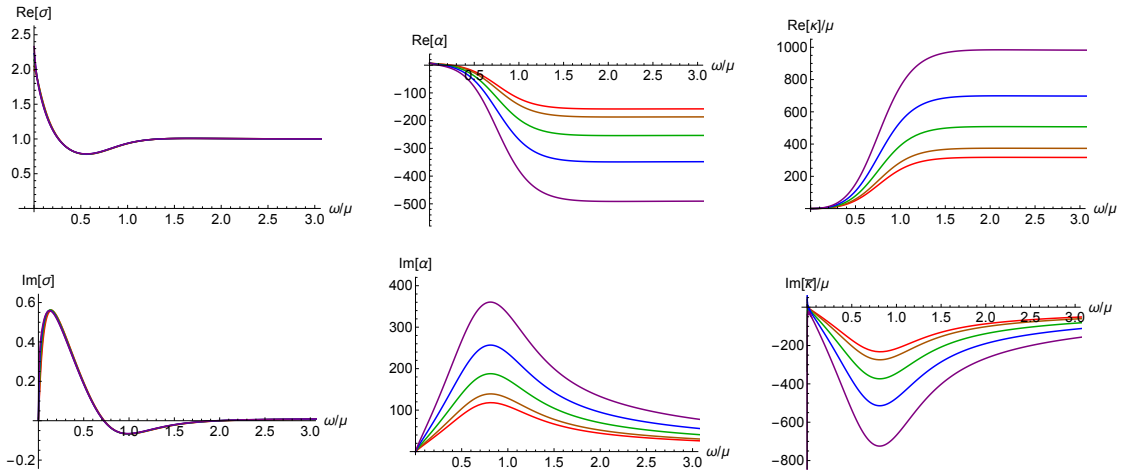

(a) Electric conductivity **(b)** Thermoelectric conductivity **(c)** Thermal conductivity

Figure 3. AC electric conductivity($\sigma(\omega)$), thermoelectric conductivity($\alpha(\omega)$), and thermal conductivity($\bar{\kappa}(\omega)$) for $\beta/\mu = 1$ and $q = 0$ at different temperatures: $T/T_c = 1, 0.84, 0.62, 0.45, 0.32$ (red, orange,green, blue). Top is the real part and bottom is the imaginary part of conductivities.

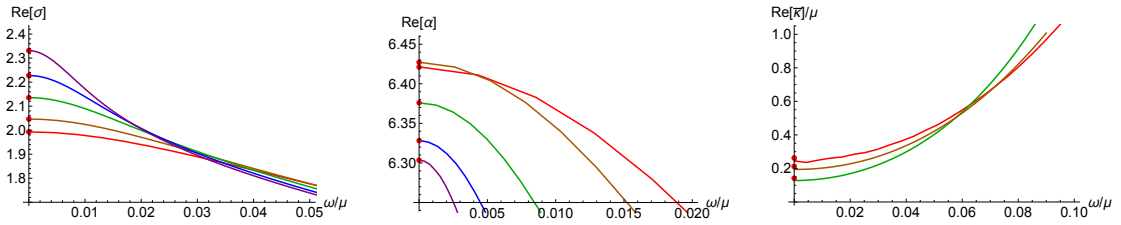

Figure 4. Near $\omega = 0$ behaviours of the real part of conductivities in figure 3.

To have an instability at $q = 0$ we choose the same parameters as figure 2: $m^2 = -2$ and $\beta/\mu = 1$. For $q = 0$, $m^2_{\text{eff}} = -1/2$, which is below the BF bound (3.1). Figure 3 shows our numerical results of conductivites, where all temperatures are below T_c: $T/T_c = 1, 0.84, 0.62, 0.45, 0.32$ for red, orange,green, and blue curves respectively. A main difference of figure 3 from figure 2 is the disappearance of $1/\omega$ pole in $\text{Im}[\sigma]$ below T_c. It confirms that the neutral scalar hair has nothing to do with superconductivity as expected.

In figure 3 it is not easy to see the conductivities in small ω regime, so we zoom in there in figure 4. Contrary to the conductivity of normal component in superconducting phase, the DC electric conductivity is not so sensitive to temperature and increases as temperature decreases, which is the property of metal. The thermoelectric and thermal conductivities decrease as temperature increases except a small increase of thermoelectric conductivity near the critical temperature. As a cross check, we have also computed these DC conductivities analytically by using the black hole horizon data according to the method developed in [52]. Since there is no singular behavior in the conductivities as $\omega \to 0$ we may regard the real scalar field here as the dilaton in [52] and the conductivities read

$$\sigma = 1 + \frac{4\pi\mathcal{Q}^2}{\beta^2 s}\,, \qquad \alpha = 4\pi\frac{\mathcal{Q}}{\beta^2}\,, \qquad \bar{\kappa} = 4\pi\frac{sT}{\beta^2}\,, \tag{3.3}$$

JHEP10(2016)041

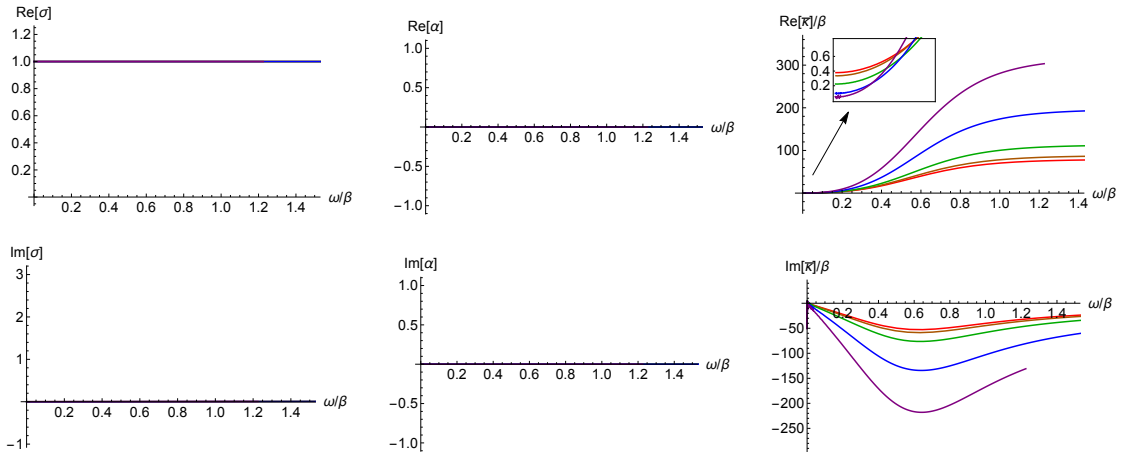

(a) Electric conductivity **(b)** Thermoelectric conductivity **(c)** Thermal conductivity

Figure 5. AC electric conductivity($\sigma(\omega)$), thermoelectric conductivity($\alpha(\omega)$), and thermal conductivity($\bar{\kappa}(\omega)$) for $\mu = 0$ and $q = 0$ at different temperatures: $T/T_c = 1, 0.9, 0.7, 0.4, 0.25$ (red, orange,green, blue, purple). Top is the real part and bottom is the imaginary part of conductivities.

where s, $\mathcal{Q}$ and T are the entropy density, charge density and temperature in the dual field theory. They are given by $s = 4\pi r_h^2$, $\mathcal{Q} = \lim_{r\to\infty} r^2 e^{\chi/2} A_t'(r)$ and $T = \frac{U'(r_h)}{4\pi} e^{(\chi(\infty)-\chi(r_h))/2}$. The analytic values are designated by the red dots in figure 4 and they agree to the numerical values very well. For a special case with $\mu = 0$, in figure 5, we see that $\sigma(\omega) = 1$, different from superconducting case ($q \neq 0$ shown in [46]), but $\alpha(\omega) = 0$, same as superconducting case.

3.3 General expression for superfluid density

We have found that for $q = 0$ there is no $1/\omega$ pole in $\mathrm{Im}[\sigma]$, of which strength corresponds to superfluid density. To understand it better, we derive an expression for superfluid density for $q \neq 0$. Let us start with the Maxwell equation,

$$\nabla_M F^{MN} = -iq\left(\Phi^* D^N \Phi - \Phi D^N \Phi^*\right) . \tag{3.4}$$

Once we assume that all fields depend on r and t and the fluctuations are allowed only for the x-direction, the x-component of the Maxwell equation reads

$$\partial_r \sqrt{-g} F^{xr} = \partial_t \sqrt{-g} F^{tx} + iq\sqrt{-g}\left(\Phi^* D^x \Phi - \Phi D^x \Phi^*\right) . \tag{3.5}$$

The integration of (3.5) from horizon to boundary gives the boundary current

$$\begin{aligned} J^x &\equiv \lim_{r\to\infty} \sqrt{-g} F^{xr} \\ &= \lim_{r\to r_h} \sqrt{-g} F^{xr} + \int_{r_h}^{\infty} \mathrm{d}r \partial_t \sqrt{-g} F^{tx} + iq \int_{r_h}^{\infty} \mathrm{d}r \sqrt{-g}\left(\Phi^* D^x \Phi - \Phi D^x \Phi^*\right) . \end{aligned} \tag{3.6}$$

JHEP10(2016)041

By hydrodynamic expansion for small ω, it turns out that the first term and the second term goes to zero as[8]

$$\lim_{r\to r_h}\sqrt{-g}F^{xr}\sim\mathcal{O}(\omega)e^{-i\omega t}\,,\qquad \int_{r_h}^{\infty}\mathrm{d}r\partial_t\sqrt{-g}F^{tx}\sim\mathcal{O}(\omega^2)e^{-i\omega t}\,, \tag{3.8}$$

while the last term goes to constant. Here we used the expression of the fields near horizon

$$\begin{aligned}
\delta A_x &= \left(\frac{\mathrm{U}(r)}{r^2}\right)^{-i\frac{\omega}{4\pi T}}\hat{a}_x(\omega,r)e^{-i\omega t}\,,\\
\delta g_{tx} &= r^2\left(\frac{\mathrm{U}(r)}{r^2}\right)^{-i\frac{\omega}{4\pi T}}\hat{h}_x(\omega,r)e^{-i\omega t}+i\omega r^2\zeta e^{-i\omega t}\,,\\
\delta\psi_x &= \left(\frac{\mathrm{U}(r)}{r^2}\right)^{-i\frac{\omega}{4\pi T}}\hat{\xi}_x(\omega,r)e^{-i\omega t}+\beta\zeta e^{-i\omega t}\,,
\end{aligned} \tag{3.9}$$

where ζ is a constant residual gauge parameter fixing $\delta g_{rx}=0$ [53], and $\hat{a}_x$, $\hat{h}_x$ and $\hat{\chi}_x$ can be expanded near horizon as

$$\begin{aligned}
\hat{a}_x(\omega,r)&\sim\mathcal{A}_0+\mathcal{A}_1(r-r_h)+\cdots\,,\\
\hat{h}_x(\omega,r)&\sim\mathcal{H}_1(r-r_h)+\cdots\,,\\
\hat{\xi}_x(\omega,r)&\sim\tilde{\xi}_0+\tilde{\xi}_1(r-r_h)+\cdots\,.
\end{aligned} \tag{3.10}$$

With the following source-vanishing-boundary conditions[9]

$$\lim_{r\to\infty}\frac{1}{r^2}\delta g_{tx}=\lim_{r\to\infty}(\hat{h}_x+i\omega\zeta)e^{-i\omega t}=0\,,\quad \lim_{r\to\infty}\delta\psi_x=\lim_{r\to\infty}\left(\hat{\xi}_x+\beta\zeta\right)e^{-i\omega t}=0\,, \tag{3.11}$$

except δA_x, the current (3.6) can be interpreted as

$$J^x=-i\omega\sigma_{xx}(\omega)\delta A_x|_{r=\infty}\,. \tag{3.12}$$

[8]More explicitly, by using (3.9) and (2.6), the first term of (3.8) is expressed as

$$\begin{aligned}
\sqrt{-g}F^{xr}&=\sqrt{-g}\left(F_{xr}g^{rr}g^{xx}-F_{tr}g^{rr}g^{xx}g^{tt}\delta g_{xt}\right)\\
&=-\sqrt{-g}\left(\left(-\frac{i\omega}{4\pi T}\hat{a}_x\left(\frac{U}{r^2}\right)'+\frac{U}{r^2}\hat{a}_x'+A_t'e^{\chi}\hat{h}_x\right)\left(\frac{U}{r^2}\right)^{-\frac{i\omega}{4\pi T}}+i\omega\zeta A_t'e^{\chi}\right)e^{-i\omega t}\,,
\end{aligned}$$

where at horizon the second term and third term vanishes because $\mathrm{U}(r_h)=0$ and $\hat{h}_x\sim(r-r_h)$ (3.10). Thus, $\lim_{r\to r_h}\sqrt{-g}F^{xr}\sim\mathcal{O}(\omega)e^{-i\omega t}$. Similarly, by using (3.9) and (2.6), the second term of (3.8) is expressed as

$$\int_{r_h}^{\infty}\mathrm{d}r\partial_t\sqrt{-g}F^{tx}=\int_{r_h}^{\infty}\mathrm{d}r\sqrt{-g}g^{tt}g^{xx}\partial_t^2\delta A_x=\omega^2\int_{r_h}^{\infty}\mathrm{d}r\frac{e^{\frac{\chi}{2}}}{U}\left(\frac{U}{r^2}\right)^{-i\frac{\omega}{4\pi T}}\hat{a}_xe^{-i\omega t}\,, \tag{3.7}$$

which is of order ω^2.

[9]The source-vanishing condition is equivalent to the relation $\omega\hat{\xi}_x(\infty)=i\beta\hat{h}_x(\infty)$. Thus it will give some constraint between two fields $\hat{\xi}_x$ and $\hat{h}_x$ near horizon, but it does not affect (3.8) because $\hat{\xi}_x$ does not enter in counting order ω near horizon as shown in footnote 8.

JHEP10(2016)041

Because only the last term of (3.6) contribute to J^x for $\omega = 0$, as discussed in (3.8), the superfluid density K_s(the strength of the $1/\omega$ pole of Im$[\sigma]$) is given by

$$\begin{aligned} K_s &\equiv \lim_{\omega\to 0} \omega \mathrm{Im}[\sigma] = \lim_{\omega\to 0} \frac{J^x}{\delta A_x(r=\infty)} \\ &= \lim_{\omega\to 0} \frac{iq}{\delta A_x(r=\infty)} \int_{r_h}^{\infty} \mathrm{d}r \sqrt{-g} \left(\Phi^* D^x \Phi - \Phi D^x \Phi^*\right) \\ &= \lim_{\omega\to 0} \frac{2q^2}{\delta A_x(r=\infty)} \int_{r_h}^{\infty} \mathrm{d}r e^{-\chi/2} |\Phi|^2 \left(\delta A_x + \frac{A_t}{\mathrm{U}(r)} e^{\chi} \delta g_{tx}\right) . \end{aligned} \tag{3.13}$$

This shows how the hairy configuration Φ contributes to K_s. If $q = 0$, K_s vanishes, which confirms our numerical analysis.

4 Ward identities: constraints between conductivities

In this section, our goals are threefold. First, we derive the constraints between three conductivities (electric, thermoelectric, and thermal) in superconducting phase with momentum relaxation, which generalize the constraints in normal phase without momentum relaxation computed in [3, 55]. These constraints are obtained analytically from field theory perspective, by analyzing the Ward identities. Second, we confirm the constraints numerically from holographic perspective, by solving bulk equations numerically. This confirmation serves as a nice cross-check of our holographic computation and numerical method. Third, we compute the small ω limit of the constraints and identify superfluid density and normal fluid density and the relation between them.

In section 4.1 we analytically derive the Ward identities for our model (2.1) with $q \neq 0$ regarding diffeomorphism from field theory perspective. In our field theoretic derivation of the Ward identities, we do not use any details of the bulk model except field contents, so they hold in more general models sharing the same symmetry and field contents as our specific model (2.1). The minimum requirement is that the system should be invariant under diffeomorphism and U(1) gauge transformation (without gravitational and gauge anomalies). In addition, we assume that the system is described by the following operators: the stress-energy tensor $T^{\alpha\beta}$, U(1) current J^μ, two real scalar operators $\mathcal{O}^I (I = 1, 2)$, and complex operators $\mathcal{O}_\Phi, {\mathcal{O}_\Phi}^\dagger$. Therefore, we will introduce the corresponding external sources: metric $\bar{h}_{\alpha\beta}$, the gauge field $\bar{A}_\mu$, real scalar sources $\bar{\psi}_I$, and complex scalar sources $\bar{\Phi}^*$,$\bar{\Phi}$ respectively.

By using specific field theory information of our model, general Ward identities boil down to constraints between conductivities$(\sigma, \alpha, \bar{\kappa})$ and two-point functions related to the scalar operator. Our main results are (4.44)–(4.45) for finite magnetic field ($B \neq 0$) and (4.56)–(4.58) for zero magnetic field ($B = 0$). They extend the Ward identities for normal phase without momentum relaxation [3, 55] to superconducting phase with momentum relaxation. Next, in section 4.2 we confirm them numerically from holographic perspective, by solving bulk equations numerically.

JHEP10(2016)041

4.1 Analytic derivation: field theory

To derive the Ward identities, we closely follow the procedure in [3][10] and extend the results therein to the case with real and complex scalar fields, which are $\bar{\psi}_I$ and $\bar{\Phi}$ in (4.1). Our final results are (4.44)–(4.45) and (4.56)–(4.58).

Let us start with a generating functional for Euclidean time ordered correlation functions:

$$e^{W[\bar{h}_{\alpha\beta},\bar{A}_\mu,\bar{\psi}_I,\bar{\Phi},\bar{\Phi}^*]} = \int DX e^{-S[X,\bar{h}_{\alpha\beta},\bar{A}_\mu,\bar{\psi}_I,\bar{\Phi},\bar{\Phi}^*]}\,, \tag{4.1}$$

where $\bar{h}_{\alpha\beta}$, $\bar{A}_\mu$, $\bar{\psi}_I$, $\bar{\Phi}$, and $\bar{\Phi}^*$ are the non-dynamical external sources of the stress-energy tensor $T^{\alpha\beta}$, U(1) current J^μ, real scalar operators $\mathcal{O}^J$, and complex operators ${\mathcal{O}_\Phi}^\dagger, \mathcal{O}_\Phi$ respectively. We define the one-point functions by functional derivatives of W:

$$\langle J^\mu(x)\rangle = \frac{\delta W}{\delta \bar{A}_\mu(x)}\,,\quad \langle T^{\mu\nu}(x)\rangle = 2\frac{\delta W}{\delta \bar{h}_{\mu\nu}(x)}\,,\quad \left\langle \mathcal{O}^I(x)\right\rangle = \frac{\delta W}{\delta \bar{\psi}_I(x)}\,,\quad \langle \mathcal{O}_\Phi(x)\rangle = \frac{\delta W}{\delta \bar{\Phi}(x)^*}\,, \tag{4.2}$$

where these expectation values are not tensors but tensor densities under diffeomorphism. One more functional derivatives acting on one-pint functions give us Euclidean time ordered ($\mathcal{P}_t$) two-point functions:

$$G_E^{\mu\nu,\alpha\beta}(x,y) \equiv \left\langle \mathcal{P}_t(T^{\mu\nu}(x)T^{\alpha\beta}(y))\right\rangle = 4\frac{\delta^2 W}{\delta\bar{h}_{\mu\nu}(x)\delta\bar{h}_{\alpha\beta}(y)}\,, \tag{4.3}$$

$$G_E^{\mu\nu,\alpha}(x,y) \equiv \langle \mathcal{P}_t(T^{\mu\nu}(x)J^{\alpha}(y))\rangle = 2\frac{\delta^2 W}{\delta\bar{h}_{\mu\nu}(x)\delta\bar{A}_{\alpha}(y)}\,, \tag{4.4}$$

$$G_E^{\mu\nu,I}(x,y) \equiv \left\langle \mathcal{P}_t(T^{\mu\nu}(x)\mathcal{O}^I(y))\right\rangle = 2\frac{\delta^2 W}{\delta\bar{h}_{\mu\nu}(x)\delta\bar{\psi}_I(y)}\,, \tag{4.5}$$

$$G_E^{\mu\nu,\Phi}(x,y) \equiv \left\langle \mathcal{P}_t(T^{\mu\nu}(x)\mathcal{O}^\Phi(y))\right\rangle = 2\frac{\delta^2 W}{\delta\bar{h}_{\mu\nu}(x)\delta\bar{\Phi}^*(y)}\,, \tag{4.6}$$

$$G_E^{\mu,\alpha}(x,y) \equiv \langle \mathcal{P}_t(J^{\mu}(x)J^{\alpha}(y))\rangle = \frac{\delta^2 W}{\delta\bar{A}_{\mu}(x)\delta\bar{A}_{\alpha}(y)}\,, \tag{4.7}$$

$$G_E^{\mu,I}(x,y) \equiv \left\langle \mathcal{P}_t(J^{\mu}(x)\mathcal{O}^I(y))\right\rangle = \frac{\delta^2 W}{\delta\bar{A}_{\mu}(x)\delta\bar{\psi}_I(y)}\,, \tag{4.8}$$

$$G_E^{\mu,\Phi}(x,y) \equiv \left\langle \mathcal{P}_t(J^{\mu}(x)\mathcal{O}^\Phi(y))\right\rangle = \frac{\delta^2 W}{\delta\bar{A}_{\mu}(x)\delta\bar{\Phi}^*(y)}\,, \tag{4.9}$$

$$G_E^{J,I}(x,y) \equiv \left\langle \mathcal{P}_t(\mathcal{O}^J(x)\mathcal{O}^I(y))\right\rangle = \frac{\delta^2 W}{\delta\bar{\psi}_J(x)\delta\bar{\psi}_I(y)}\,, \tag{4.10}$$

$$G_E^{J,\Phi}(x,y) \equiv \left\langle \mathcal{P}_t(\mathcal{O}^J(x)\mathcal{O}^\Phi(y))\right\rangle = \frac{\delta^2 W}{\delta\bar{\psi}_J(x)\delta\bar{\Phi}^*(y)}\,, \tag{4.11}$$

$$G_E^{\Phi,\Phi^*}(x,y) \equiv \left\langle \mathcal{P}_t(\mathcal{O}^\Phi(x)\mathcal{O}^{\Phi\,\dagger}(y))\right\rangle = \frac{\delta^2 W}{\delta\bar{\Phi}^*(x)\delta\bar{\Phi}(y)}\,. \tag{4.12}$$

We consider the generating functional $W[\bar{h}_{\alpha\beta},\bar{A}_\mu,\bar{\psi}_I,\bar{\Phi},\bar{\Phi}^*]$ invariant under diffeomorphism, $x^\mu \to x^\mu + \zeta^\mu$, and the variation of the fields can be expressed in terms of a Lie

[10] See [66] for a holographic derivation.

JHEP10(2016)041

derivative with respect to the vector field ζ_μ:

$$\delta\bar{h}_{\mu\nu} = (\mathcal{L}_\zeta \bar{h})_{\mu\nu} = \nabla_\mu \zeta_\nu + \nabla_\nu \zeta_\mu \,, \tag{4.13}$$

$$\delta\bar{A}_\mu = (\mathcal{L}_\zeta \bar{A})_\mu = \zeta^\lambda \nabla_\lambda \bar{A}_\mu + (\nabla_\mu \zeta^\nu)\bar{A}_\nu \,, \tag{4.14}$$

$$\delta\bar{\psi}_I = (\mathcal{L}_\zeta \bar{\psi}_I) = \zeta^\lambda \nabla_\lambda \psi_I \,, \tag{4.15}$$

$$\delta\bar{\Phi} = (\mathcal{L}_\zeta \bar{\Phi}) = \zeta^\lambda \nabla_\lambda \bar{\Phi} \,. \tag{4.16}$$

For diffeomorphism invariance, the variation of W should vanish:

$$\begin{aligned} \delta W = \int \mathrm{d}^3x \Bigg(& \frac{\delta W}{\delta \bar{h}_{\mu\nu}(x)} (\mathcal{L}_\zeta \bar{h})_{\mu\nu} + \frac{\delta W}{\delta \bar{A}_\mu(x)} (\mathcal{L}_\zeta \bar{A})_\mu + \frac{\delta W}{\delta \bar{\psi}_I(x)} (\mathcal{L}_\zeta \bar{\psi}_I) \\ & + \frac{\delta W}{\delta \bar{\Phi}(x)} (\mathcal{L}_\zeta \bar{\Phi}) + \frac{\delta W}{\delta \bar{\Phi}^*(x)} (\mathcal{L}_\zeta \bar{\Phi}^*) \Bigg) = 0 \,, \end{aligned} \tag{4.17}$$

which, after integration by parts, yields the Ward identity for one-point functions regarding diffeomorphism.

$$D_\mu \langle T^{\mu\nu} \rangle + \bar{F}_\lambda{}^\nu \langle J^\lambda \rangle + \langle \mathcal{O}^I \rangle \bar{h}^{\nu\lambda} \partial_\lambda \bar{\psi}_I + \langle \mathcal{O}^\Phi \rangle \bar{h}^{\nu\lambda} \partial_\lambda \bar{\Phi}^* + \langle \mathcal{O}^{\Phi\dagger} \rangle \bar{h}^{\nu\lambda} \partial_\lambda \bar{\Phi} = 0 \,, \tag{4.18}$$

where $D_\mu \langle T^{\mu\nu}(x) \rangle \equiv \partial_\mu \langle T^{\mu\nu}(x) \rangle + \Gamma^\nu_{\alpha\beta} \langle T^{\alpha\beta}(x) \rangle$. Here we also used the Ward identity for U(1) gauge symmetry, which is summarized in footnote 12.

By taking a derivative of (4.18) with respect to either $\bar{h}_{\alpha\beta}(y)$, $\bar{A}_\alpha(y)$, $\bar{\psi}^J(y)$ or $\bar{\Phi}^*(y)$, we obtain the Ward identities for the two-point functions:

$$\begin{aligned} & D_\mu \langle \mathcal{P}_t(J^\alpha(y) T^{\mu\nu}(x)) \rangle + \bar{F}_\mu{}^\nu \langle \mathcal{P}_t(J^\alpha(y) J^\mu(x)) \rangle - \bar{h}^{\nu\beta} \langle J^\alpha(x) \rangle \frac{\partial}{\partial x^\beta} \delta(x-y) \\ & + \bar{h}^{\nu\alpha} \langle J^\mu(x) \rangle \frac{\partial}{\partial x^\mu} \delta(x-y) + \bar{h}^{\mu\nu} \partial_\mu \bar{\psi} \langle \mathcal{P}_t(J^\alpha(y) \mathcal{O}^I(x)) \rangle \\ & + 2\mathrm{Re} \left\{ \bar{h}^{\mu\nu} \partial_\mu \bar{\Phi}^* \langle \mathcal{P}_t(J^\alpha(y) \mathcal{O}^\Phi(x)) \rangle \right\} = 0 \,, \end{aligned} \tag{4.19}$$

$$\begin{aligned} & D_\mu \left\langle \mathcal{P}_t(T^{\alpha\beta}(y) T^{\mu\nu}(x)) \right\rangle + \delta(x-y) \left(\bar{h}^{\nu\alpha} D_\mu \left\langle T^{\mu\beta}(x) \right\rangle + g^{\nu\beta} D_\mu \langle T^{\mu\alpha}(x) \rangle \right) \\ & + \left(g^{\nu\alpha} \left\langle T^{\mu\beta}(x) \right\rangle + \bar{h}^{\nu\beta} \langle T^{\mu\alpha}(x) \rangle - \bar{h}^{\mu\nu} \left\langle T^{\alpha\beta}(x) \right\rangle \right) \frac{\partial}{\partial x^\mu} \delta(x-y) \\ & - \left(\bar{h}^{\nu\alpha} \Gamma^\beta_{\mu\lambda} + \bar{h}^{\nu\beta} \Gamma^\alpha_{\mu\lambda} \right) \left\langle T^{\mu\lambda}(x) \right\rangle \delta(x-y) \\ & + \bar{h}^{\nu\mu} \left(\bar{F}_{\mu\lambda} \left\langle \mathcal{P}_t(T^{\alpha\beta}(y) J^\lambda(x)) \right\rangle - \partial_\mu \bar{\psi}_I \left\langle \mathcal{P}_t(T^{\alpha\beta}(y) \mathcal{O}^I(x)) \right\rangle \right) \\ & - 2\mathrm{Re} \left\{ \bar{h}^{\nu\mu} \partial_\mu \bar{\Phi}^* \left\langle \mathcal{P}_t(T^{\alpha\beta}(y) \mathcal{O}^\Phi(x)) \right\rangle \right\} = 0 \,, \end{aligned} \tag{4.20}$$

$$\begin{aligned} & D_\mu \langle \mathcal{P}_t(\mathcal{O}^J(y) T^{\mu\nu}(x)) \rangle - \bar{h}^{\nu\mu} \bar{F}_{\mu\lambda} \left\langle \mathcal{P}_t(\mathcal{O}^J(y) J^\lambda(x)) \right\rangle + \bar{h}^{\nu\lambda} \langle \mathcal{P}_t(\mathcal{O}^J(y) \mathcal{O}^I(x)) \rangle \partial_\lambda \psi_I \\ & + \bar{h}^{\nu\lambda} \langle \mathcal{O}^J(x) \rangle \frac{\partial}{\partial x^\lambda} \delta(x-y) + 2\mathrm{Re} \left\{ \bar{h}^{\nu\lambda} \langle \mathcal{P}_t(\mathcal{O}^J(y) \mathcal{O}^\Phi(x)) \rangle \partial_\lambda \bar{\Phi}^* \right\} = 0 \,, \end{aligned} \tag{4.21}$$

$$\begin{aligned} & D_\mu \langle \mathcal{P}_t(\mathcal{O}^\Phi(y) T^{\mu\nu}(x)) \rangle - \bar{h}^{\nu\mu} \bar{F}_{\mu\lambda} \left\langle \mathcal{P}_t(\mathcal{O}^\Phi(y) J^\lambda(x)) \right\rangle + \bar{h}^{\nu\lambda} \langle \mathcal{P}_t(\mathcal{O}^\Phi(y) \mathcal{O}^I(x)) \rangle \partial_\lambda \bar{\psi}_I \\ & + \bar{h}^{\nu\lambda} \langle \mathcal{O}^\Phi(x) \rangle \frac{\partial}{\partial x^\lambda} \delta(x-y) + \bar{h}^{\nu\lambda} \langle \mathcal{P}_t(\mathcal{O}^\Phi(y) \mathcal{O}^\Phi(x)) \rangle \partial_\lambda \bar{\Phi}^* \\ & + \bar{h}^{\nu\lambda} \left\langle \mathcal{P}_t(\mathcal{O}^\Phi(y) \mathcal{O}^{\Phi\dagger}(x)) \right\rangle \partial_\lambda \bar{\Phi} = 0 \,, \end{aligned} \tag{4.22}$$

where the covariant derivatives act only on the operators of x.

JHEP10(2016)041

From here we consider a flat space, $\bar{h}_{\mu\nu} = \delta_{\mu\nu}$, and assume external fields such as $\bar{F}_{\mu\nu}$, $\partial_\mu \bar{\psi}_I$ and $\bar{\Phi}$, are constant in space-time. We further assume translation invariance is not spontaneously broken in the equilibrium state, so all the one point functions, $\langle T^{\mu\nu} \rangle$, $\langle J^\mu \rangle$, $\langle \mathcal{O}^I \rangle$ and $\langle \mathcal{O}^\Phi \rangle$, should be constant in space-time. In momentum space, the Ward identities (4.19)–(4.22) read

$$0 = -k_\mu \tilde{G}_E^{\alpha,\mu\nu}(k) - i\bar{F}_\mu{}^\nu \tilde{G}_E^{\alpha,\mu}(k) + k^\nu \langle J^\alpha \rangle - k_\mu \delta^{\alpha\nu} \langle J^\mu \rangle - i\delta^{\mu\nu}\partial_\mu \bar{\psi}_I \tilde{G}_E^{\alpha,I}(k)\,, \tag{4.23}$$

$$\begin{aligned} 0 = {} & k_\mu \left(\tilde{G}_E^{\alpha\beta,\mu\nu}(k) + \delta^{\nu\alpha} \left\langle T^{\mu\beta} \right\rangle + \delta^{\nu\beta} \langle T^{\mu\alpha} \rangle - \delta^{\mu\nu} \left\langle T^{\alpha\beta} \right\rangle \right) \\ & + i \left(\bar{F}_\lambda{}^\nu \tilde{G}_E^{\alpha\beta,\lambda}(k) + \delta^{\nu\mu} \partial_\mu \bar{\psi}_I \tilde{G}_E^{\alpha\beta,I}(k) \right) \\ & - i\delta^{\beta\nu} \left(\bar{F}_\mu{}^\alpha \langle J^\mu \rangle + \delta^{\alpha\lambda} \langle \mathcal{O}^I \rangle \partial_\lambda \bar{\psi}_I \right) - i\delta^{\alpha\nu} \left(\bar{F}_\mu{}^\beta \langle J^\mu \rangle + \delta^{\beta\lambda} \langle \mathcal{O}^I \rangle \partial_\lambda \bar{\psi}_I \right)\,, \end{aligned} \tag{4.24}$$

$$0 = -k_\mu \tilde{G}_E^{J,\mu\nu}(k) - i\bar{F}_\mu{}^\nu \tilde{G}_E^{J,\mu} - i\tilde{G}_E^{J,I}(k)\delta^{\nu\lambda}\partial_\lambda \bar{\psi}_I - \langle \mathcal{O}^J \rangle k^\nu\,, \tag{4.25}$$

$$0 = -k_\mu \tilde{G}_E^{\Phi,\mu\nu}(k) - i\bar{F}_\mu{}^\nu \tilde{G}_E^{\Phi,\mu} - i\tilde{G}_E^{\Phi,I}(k)\delta^{\nu\lambda}\partial_\lambda \bar{\psi}_I - \langle \mathcal{O}^\Phi \rangle k^\nu\,. \tag{4.26}$$

Since we want to study transport coefficients, we analytically continue to Minkowski space, so that the Euclidian Green's functions can be continued to the Retarded Green's functions. Thus, the Ward identities (4.23)–(4.26) become

$$0 = -k_\mu \tilde{G}_R^{\alpha,\mu\nu}(k) - i\bar{F}_\mu{}^\nu \tilde{G}_R^{\alpha,\mu}(k) + k^\nu \langle J^\alpha \rangle - k_\mu \eta^{\alpha\nu} \langle J^\mu \rangle + i\eta^{\mu\nu}\partial_\mu \bar{\psi}_I \tilde{G}_R^{\alpha,I}(k)\,, \tag{4.27}$$

$$\begin{aligned} 0 = {} & k_\mu \left(\tilde{G}_R^{\alpha\beta,\mu\nu}(k) + \eta^{\nu\alpha} \left\langle T^{\mu\beta} \right\rangle + \eta^{\nu\beta} \langle T^{\mu\alpha} \rangle - \eta^{\mu\nu} \left\langle T^{\alpha\beta} \right\rangle \right) \\ & + i \left(\bar{F}_\lambda{}^\nu \tilde{G}_R^{\alpha\beta,\lambda}(k) - \eta^{\nu\mu} \partial_\mu \bar{\psi}_I \tilde{G}_R^{\alpha\beta,I}(k) \right) \\ & - i\eta^{\beta\nu} \left(\bar{F}_\mu{}^\alpha \langle J^\mu \rangle - \eta^{\alpha\lambda} \langle \mathcal{O}^I \rangle \partial_\lambda \bar{\psi}_I \right) - i\eta^{\alpha\nu} \left(\bar{F}_\mu{}^\beta \langle J^\mu \rangle - \eta^{\beta\lambda} \langle \mathcal{O}^I \rangle \partial_\lambda \bar{\psi}_I \right)\,, \end{aligned} \tag{4.28}$$

$$0 = k_\mu \tilde{G}_R^{J,\mu\nu}(k) + i\bar{F}_\mu{}^\nu \tilde{G}_R^{J,\mu} - i\tilde{G}_R^{J,I}(k)\eta^{\nu\lambda}\partial_\lambda \bar{\psi}_I + \langle \mathcal{O}^J \rangle k^\nu\,, \tag{4.29}$$

$$0 = -k_\mu \tilde{G}_R^{\Phi,\mu\nu}(k) - i\bar{F}_\mu{}^\nu \tilde{G}_R^{\Phi,\mu} + i\tilde{G}_R^{\Phi,I}(k)\eta^{\nu\lambda}\partial_\lambda \bar{\psi}_I - \langle \mathcal{O}^\Phi \rangle k^\nu\,. \tag{4.30}$$

In particular, we consider 2+1 dimensional system in an equilibrium state with the constant expectation values for the energy-momentum and current

$$\langle T^{\mu\nu} \rangle = \begin{pmatrix} \epsilon & 0 & 0 \\ 0 & p & 0 \\ 0 & 0 & p \end{pmatrix}\,, \qquad \langle J^\mu \rangle = (n, 0, 0)\,, \tag{4.31}$$

with finite or zero condensate $\langle \mathcal{O}^\Phi \rangle$ and $\langle \mathcal{O}^I \rangle = 0$. To this system we apply a constant external magnetic field with a background scalar $\bar{\psi}_I$:

$$\bar{F} = B\mathrm{d}x \wedge \mathrm{d}y\,, \qquad \bar{\psi}_I = (\beta x, \beta y)\,. \tag{4.32}$$

We take $k^\mu = (\omega, 0, 0)$ to focus on the spatially homogeneous AC conductivity induced by the small external electric field and temperature gradient along $i(= x, y)$ direction.

Under these conditions the Ward identities (4.27)–(4.29) becomes

$$\omega \tilde{G}_R^{j,0k} - iB\epsilon^{ik}\tilde{G}_R^{j,i} + \omega\delta^{jk}n + i\beta\delta_I^k \tilde{G}_R^{j,I} = 0\,, \tag{4.33}$$

$$\omega \left(\tilde{G}_R^{0j,0k} + \delta^{kj}\epsilon \right) - i \left(B\epsilon^{ik}\tilde{G}_R^{0j,i} - \beta\delta_I^k \tilde{G}_R^{0j,I} \right) = 0\,, \tag{4.34}$$

$$-\omega \tilde{G}_R^{J,0j} + iB\epsilon^{ij}\tilde{G}_R^{J,i} - i\tilde{G}_R^{J,I}\beta\delta_I^j = 0\,, \tag{4.35}$$

JHEP10(2016)041

where i, j, k run over x and y. It is convenient to introduce the complexified combinations defined as

$$\begin{aligned}
\langle JT\rangle_\pm &\equiv \pm\tilde{G}_R^{x,0x} - i\tilde{G}_R^{x,0y}\,, & \langle JJ\rangle_\pm &\equiv \pm\tilde{G}_R^{x,x} - i\tilde{G}_R^{x,y}\,,\\
\langle TT\rangle_\pm &\equiv \pm\tilde{G}_R^{0x,0x} - i\tilde{G}_R^{0x,0y}\,, & \langle SS\rangle_\pm &\equiv \pm\tilde{G}_R^{1,1} - i\tilde{G}_R^{1,2}\,,\\
\langle SJ\rangle_\pm &\equiv \pm\tilde{G}_R^{1,x} - i\tilde{G}_R^{1,y}\,, & \langle ST\rangle_\pm &\equiv \pm\tilde{G}_R^{I=1,0x} - i\tilde{G}_R^{I=1,0y}\,.
\end{aligned} \tag{4.36}$$

With this notation, (4.33)–(4.35) can be rewritten as

$$\pm\omega\,\langle JT\rangle_\pm - B\,\langle JJ\rangle_\pm + \omega\, n \pm i\beta\,\langle JS\rangle_\pm = 0\,, \tag{4.37}$$

$$\pm\omega\,\langle TT\rangle_\pm - B\,\langle TJ\rangle_\pm + \omega\,\epsilon \pm i\beta\,\langle TS\rangle_\pm = 0\,, \tag{4.38}$$

$$\mp\omega\,\langle ST\rangle_\pm - B\,\langle SJ\rangle_\pm \mp i\beta\,\langle SS\rangle_\pm = 0\,, \tag{4.39}$$

or, in terms of the heat current $Q = T - \mu J$,

$$\pm\omega\,\langle JQ\rangle_\pm + \ (\pm\mu\omega - B)\,\langle JJ\rangle_\pm + \omega\, n \pm i\beta\,\langle JS\rangle_\pm = 0\,, \tag{4.40}$$

$$\pm\omega\,\langle QQ\rangle_\pm + \ (\pm\mu\omega - B)\,\langle JQ\rangle_\pm + \omega(\epsilon - \mu\, n) \mp i\mu\beta\,\langle JS\rangle_\pm = 0\,, \tag{4.41}$$

$$\mp\omega\,\langle SQ\rangle_\pm + \ (\mp\mu\omega - B)\,\langle SJ\rangle_\pm \mp i\beta\,\langle SS\rangle_\pm = 0\,. \tag{4.42}$$

Finally, using the Kubo formulas for conductivities[11]

$$\sigma_\pm = \frac{1}{\omega}\,\langle JJ\rangle_\pm\,, \quad \alpha_\pm = \frac{1}{\omega T}\,\langle QJ\rangle_\pm\,, \quad \bar{\alpha}_\pm = \frac{1}{\omega T}\,\langle JQ\rangle_\pm\,, \quad \bar{\kappa}_\pm = \frac{1}{\omega T}\,\langle QQ\rangle_\pm\,, \tag{4.43}$$

we obtain the relations between the conductivities:

$$\text{Ward 1}: \qquad \pm\omega^2 T\bar{\alpha}_\pm + \ \omega(\pm\mu\omega - B)\sigma_\pm + \omega\, n \pm i\beta\,\langle JS\rangle_\pm = 0\,, \tag{4.44}$$

$$\text{Ward 2}: \quad \pm\omega^2 T\bar{\kappa}_\pm + \ \omega(\pm\mu\omega - B)T\bar{\alpha}_\pm + \omega(\epsilon' - \mu\, n) \mp i\mu\beta\,\langle JS\rangle_\pm = 0\,, \tag{4.45}$$

$$\text{Ward 3}: \qquad \mp\omega\,\langle SQ\rangle_\pm + \ (\mp\mu\omega - B)\,\langle SJ\rangle_\pm \mp i\beta\,\langle SS\rangle_\pm = 0\,, \tag{4.46}$$

where we redefined $\bar{\kappa}_\pm$

$$\bar{\kappa}_\pm \to \bar{\kappa}_\pm - \frac{\langle TT\rangle_{\pm,\omega=0}}{\omega T}\,, \tag{4.47}$$

to subtract a counter term and $\epsilon' \equiv \epsilon \pm \langle TT\rangle_{\pm,\omega=0}$. In normal phase, if $\beta = 0$ and $B \neq 0$, $\langle TT\rangle_{\pm,\omega=0} = \pm\epsilon/2$ [3].

If $B = 0$, (4.37)–(4.39) is simplified as

$$\omega\,\langle JT\rangle + \omega\, n + i\beta\,\langle JS\rangle = 0\,, \tag{4.48}$$

$$\omega\,\langle TT\rangle + \omega\,\epsilon + i\beta\,\langle TS\rangle = 0\,, \tag{4.49}$$

$$\omega\,\langle ST\rangle + i\beta\,\langle SS\rangle = 0\,, \tag{4.50}$$

where

$$\begin{aligned}
\langle JT\rangle &\equiv \tilde{G}_R^{x,0x}\,, & \langle JS\rangle &\equiv \tilde{G}_R^{x,1}\,, & \langle TT\rangle &\equiv \tilde{G}_R^{0x,0x}\,,\\
\langle TS\rangle &\equiv \tilde{G}_R^{0x,1}\,, & \langle ST\rangle &\equiv \tilde{G}_R^{1,0x}\,, & \langle SS\rangle &\equiv \tilde{G}_R^{1,1}\,,
\end{aligned} \tag{4.51}$$

[11] The complexified conductivities are denoted by $X_\pm \equiv X_{xy} \pm iX_{xx}$, where $X = \sigma, \alpha, \bar{\alpha}, \bar{\kappa}$.

JHEP10(2016)041

since we don't need to consider y-coordinate. Or, in terms of the heat current $Q = T - \mu J$,

$$\langle JQ\rangle + \mu\langle JJ\rangle + n + i\frac{\beta}{\omega}\langle JS\rangle = 0\,, \tag{4.52}$$

$$\langle QQ\rangle + \mu\langle JQ\rangle + \mu\langle QJ\rangle + \mu^2\langle JJ\rangle + \epsilon + i\frac{\beta}{\omega}(\langle QS\rangle + \mu\langle JS\rangle) = 0\,, \tag{4.53}$$

$$\langle SQ\rangle + \mu\langle SJ\rangle + n + i\frac{\beta}{\omega}\langle SS\rangle = 0\,. \tag{4.54}$$

Using the Kubo formulas

$$\sigma = \frac{1}{i\omega}\langle JJ\rangle\,,\quad \alpha = \frac{1}{i\omega T}\langle QJ\rangle\,,\quad \bar{\alpha} = \frac{1}{i\omega T}\langle JQ\rangle\,,\quad \bar{\kappa} = \frac{1}{i\omega T}\langle QQ\rangle\,, \tag{4.55}$$

we obtain the relations between the conductivities:

$$\text{Ward 4}: \qquad \alpha + \frac{\mu}{T}\sigma - i\frac{n}{\omega T} + \beta\frac{\langle JS\rangle}{\omega^2 T} = 0\,, \tag{4.56}$$

$$\text{Ward 5}: \quad \bar{\kappa} + 2\mu\alpha + \frac{\mu^2\sigma}{T} - i\frac{\epsilon'}{\omega T} + \beta\frac{\langle QS\rangle}{\omega^2 T} + \beta\frac{\mu\langle JS\rangle}{\omega^2 T} = 0\,, \tag{4.57}$$

$$\text{Ward 6}: \qquad \langle ST\rangle + i\beta\frac{\langle SS\rangle}{\omega} = 0\,, \tag{4.58}$$

where $\bar{\kappa}$ is redefined as (4.47) to subtract a counter term and $\epsilon' = \epsilon + \langle TT\rangle_{\omega=0}$. In normal phase, $\langle TT\rangle_{\omega=0} = -\epsilon$ and $\epsilon/2$ for $\beta = 0$ and $\beta \neq 0$ respectively. In superconducting phase for $\beta = 0$, $\langle TT\rangle_{\omega=0} = -\epsilon$.[12]

4.2 Numerical confirmation: holography

In the previous subsection we have derived the Ward identities for two-point functions from field theory perspective. Here we show that those Ward identities indeed hold in our holographic model studied in [31, 46, 54]. More concretely, our goal is to compute $\sigma, \alpha, \bar{\kappa}, \langle JS\rangle, \langle QS\rangle, \langle SS\rangle$ numerically and plug them into the Ward identities (4.44)–(4.45) and (4.56)–(4.58) to check if they add up to zero or not.

For $B = 0$, the conductivities $\sigma, \alpha, \bar{\kappa}$ were reported in [54] and reproduced in figure 2. Here in figure 6 we display the other two-point correlation functions related to the real scalar operator, $\langle JS\rangle$, $\langle QS\rangle$, and $\langle SS\rangle$. Contrary to figure 2 there is no divergence at $\omega = 0$, which is also shown in their small ω expressions (4.68)–(4.70). By using the data in figure 2 and 6 we numerically compute the left hand side of three Ward identities (4.56)–(4.58). The numerical sums for all considered temperatures are shown together in figure 7. All of them vanish($< 10^{-15}$), confirming analytic formulas. We have also checked three other cases: 1) $B = 0$ and $\beta/\mu = 0.1$, 2) $B = 0$ and $\mu = 0$, 3) $B \neq 0$. It turned out that all numerical sums vanish too. For completeness, we show the numerical data for these three cases in the appendix A.

[12] If W is invariant under U(1) gauge transformations, $\bar{A}_\mu \to \bar{A}_\mu + \partial_\mu\Lambda$, the Ward identity for one-point function yields current conservation $\partial_\mu\langle J^\mu(x)\rangle = 0$. The Ward identities for two point functions are $-\omega G^{t,t} + kG^{t,x} = 0, -\omega G^{t,x} + kG^{x,x} = 0, -\omega G^{\Phi,t} + kG^{\Phi,x} = \langle\mathcal{O}^\Phi\rangle, -\omega G^{\bar{\Phi},t} + kG^{\bar{\Phi},x} = -\langle\mathcal{O}^\Phi\rangle$, [67] and $-\omega G^{1,t} + kG^{1,x} = 0$.

JHEP10(2016)041

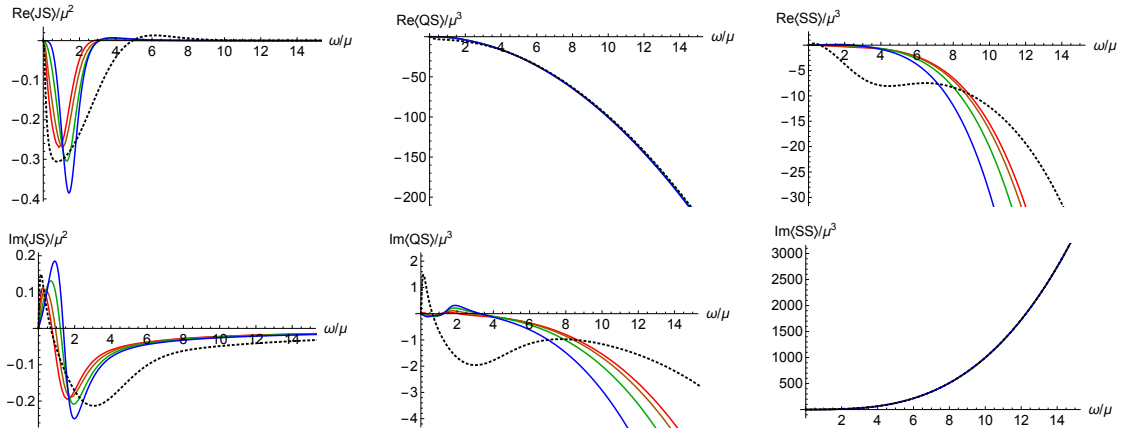

Figure 6. $\langle JS\rangle$, $\langle QS\rangle$, $\langle SS\rangle$ for $\mu/\beta = 1$ at $T/T_c = 3.2, 1, 0.89, 0.66, 0.27$ (dotted, red, orange, green, blue).

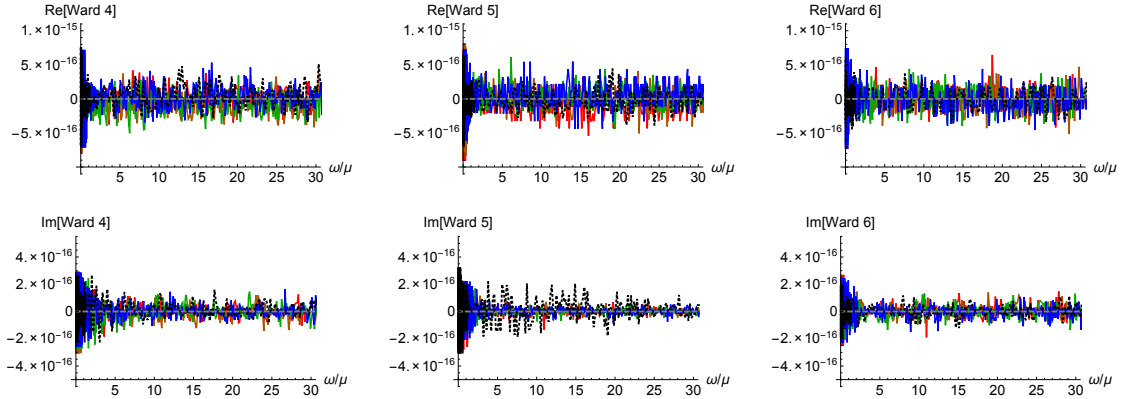

(a) Ward 4: (4.56) **(b)** Ward 5: (4.57) **(c)** Ward 6: (4.58)

Figure 7. Confirmation of Ward identities. The left hand side of (4.56)–(4.58) is plotted for the temperatures shown in figure 6 all together. They are almost zero, less than 10^{-15}.

4.3 Conductivities at small ω

In this subsection we analyse small ω behaviours of the two-point correlation functions based on our numerical results and Ward Identities both in superconducting and normal phase. After identifying superfluid density and normal component density in the two fluid model of superconductor we check Homes' law and Uemura's law.

For $\beta = 0$, the Ward identities (4.56)–(4.58) become simplified

$$\begin{aligned} \mathrm{Re}[\alpha] &= -\frac{\mu}{T}\mathrm{Re}[\sigma]\,, & \mathrm{Re}[\bar{\kappa}] &= -\mu\mathrm{Re}[\alpha]\,, \\ \mathrm{Im}[\alpha] + \frac{\mu}{T}\mathrm{Im}[\sigma] &= \frac{n}{\omega T}\,, & \mathrm{Im}[\bar{\kappa}] + \mu\mathrm{Im}[\alpha] &= \frac{\epsilon' - \mu\, n}{\omega T}\,. \end{aligned} \tag{4.59}$$

This relation was reported in [2] for normal phase and here we have shown it still holds for superconducting phase. By these relations, once σ is obtained, α and $\bar{\kappa}$ are completely determined. In both normal and superconducting phase, $\mathrm{Im}[\sigma]$ turns out to have $1/\omega$ pole by numerical computation so $\mathrm{Re}[\sigma]$ is infinite by the Kramers-Kronig relation [2, 8, 31].

JHEP10(2016)041

Therefore, by (4.59), Re[α] and Re[$\bar{\kappa}$] are also infinite and Im[α] and Im[$\bar{\kappa}$] have $1/\omega$ poles. In normal phase it is due to the absence of momentum relaxation and in superconducting phase there is another contribution due to condensate.

For $\beta \neq 0$, the Ward identities (4.56)–(4.58) may be rewritten as

$$\mathrm{Re}[\alpha] + \frac{\mu}{T}\mathrm{Re}[\sigma] = -\frac{\beta}{T}\frac{\mathrm{Re}[\langle JS\rangle]}{\omega^2}\,, \tag{4.60}$$

$$\mathrm{Im}[\alpha] + \frac{\mu}{T}\mathrm{Im}[\sigma] = \frac{n}{\omega T} - \frac{\beta}{T}\frac{\mathrm{Im}[\langle JS\rangle]}{\omega^2}\,, \tag{4.61}$$

$$\mathrm{Re}[\bar{\kappa}] + \mu\mathrm{Re}[\alpha] = -\frac{\beta}{T}\frac{\mathrm{Re}[\langle QS\rangle]}{\omega^2}\,, \tag{4.62}$$

$$\mathrm{Im}[\bar{\kappa}] + \mu\mathrm{Im}[\alpha] = \frac{\epsilon'}{\omega T} - \frac{\mu\, n}{\omega T} - \frac{\beta}{T}\frac{\mathrm{Im}[\langle QS\rangle]}{\omega^2}\,, \tag{4.63}$$

$$\langle QS\rangle + \mu\,\langle JS\rangle + \beta\frac{\langle SS\rangle}{\omega} = 0\,, \tag{4.64}$$

where (4.62) and (4.63) are obtained by combining (4.56) and (4.57), and we used $Q = T - \mu J$. Contrary to the case of $\beta = 0$, α and $\bar{\kappa}$ are not determined by σ only, because there are other correlators $\langle JS\rangle$, $\langle QS\rangle$, and $\langle SS\rangle$ involved in the Ward Identities. For exmaple, once we know σ, α, and $\bar{\kappa}$, we can read off $\langle JS\rangle$, $\langle QS\rangle$, and $\langle SS\rangle$ by the Ward identities.

In normal phase (see, for example, the dotted curve in figure 2), the real and imaginary part of σ, α, and $\bar{\kappa}$ are all finite at $\omega = 0$ due to the momentum relaxation ($\beta \neq 0$). At small ω, it is inferred that $\mathrm{Re}[\langle JS\rangle] \sim \omega^2$ from (4.60) and $\mathrm{Im}[\langle JS\rangle] \sim \omega$ from (4.61). Also $\mathrm{Re}[\langle QS\rangle] \sim \omega^2$ from (4.62) and $\mathrm{Im}[\langle QS\rangle] \sim \omega$ from (4.63).[13] Finally, the small ω behaviour of $\langle SS\rangle$ is determined by $\langle JS\rangle$ and $\langle QS\rangle$ via (4.64). In superconducting phase (see for example the solid curves in figure 2), unlike normal phase, Im[σ] and Im[$\bar{\kappa}$] have $1/\omega$ poles, which implies the existence of delta functions at $\omega = 0$ in the corresponding real parts. In summary, the small ω behaviours can be written as

$$\sigma \sim K_s\frac{\pi}{2}\delta(\omega) + \sigma_{\mathrm{DC}} + i\left(\frac{K_s}{\omega} + \omega\sigma_I\right), \tag{4.65}$$

$$\alpha \sim \alpha_{\mathrm{DC}} + i\omega\alpha_I, \tag{4.66}$$

$$\bar{\kappa} \sim -\frac{\mu^2 K_s}{T}\frac{\pi}{2}\delta(\omega) + \bar{\kappa}_{\mathrm{DC}} + i\left(-\frac{\mu^2 K_s}{T}\frac{1}{\omega} + \omega\bar{\kappa}_I\right), \tag{4.67}$$

$$\langle JS\rangle \sim \frac{1}{\beta}\left(-\mu K_s\frac{\pi}{2}\delta(\omega) - \mu\sigma_{\mathrm{DC}} - T\alpha_{\mathrm{DC}}\right)\omega^2 + i\omega\left(\frac{n-\mu K_s}{\beta}\right), \tag{4.68}$$

$$\langle QS\rangle \sim \frac{1}{\beta}\left(\mu^2 K_s\frac{\pi}{2}\delta(\omega) - T\kappa_{\mathrm{DC}} - \mu T\alpha_{\mathrm{DC}}\right)\omega^2 + i\omega\left(\frac{\epsilon' - \mu(n-\mu K_s)}{\beta}\right), \tag{4.69}$$

$$\langle SS\rangle \sim -\frac{\epsilon'}{\beta^2}\omega^2 + i\omega^3\frac{T}{\beta^2}\left(-\kappa_{\mathrm{DC}} - 2\mu\alpha_{\mathrm{DC}} - \frac{\mu^2}{T}\sigma_{\mathrm{DC}}\right), \tag{4.70}$$

where $\sigma_{\mathrm{DC}}, \alpha_{\mathrm{DC}}, \bar{\kappa}_{\mathrm{DC}}$ are real value of conductivities at $\omega = 0$, while $\sigma_I, \alpha_I, \bar{\kappa}_I$ are imaginary values linear to ω. K_s is introduced as a strength of the pole of Im[σ],

$$K_s = \lim_{\omega\to 0}\omega\mathrm{Im}[\sigma]\,, \tag{4.71}$$

[13] It is possible that the power of ω could be bigger than what are inferred. We have fixed them from numerical data.

JHEP10(2016)041

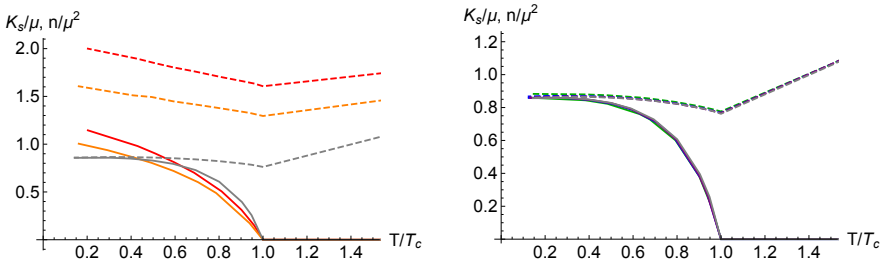

(a) $\frac{\mu}{\beta} = 0.3, 0.4, 10$ (red, orange, gray) **(b)** $\frac{\mu}{\beta} = 3, 5, 7, 10$ (green, blue, purple, gray)

Figure 8. $\frac{n}{\mu^2}$(dotted curves) and $\frac{K_s}{\mu}$(solid curves) for $q = 3$: the normal density K_n/μ at a given μ/β is the difference between the dotted and solid curve. The K_n at low temperature vanishes when $\frac{\mu}{\beta} \gtrsim 2$.

which can be identified with the superfluid density [42]. In (4.65)–(4.70), K_s is the only parameter characterising the superconducting phase and if we set $K_s = 0$ the expressions works for the normal phase. The two-point functions related to the scalar operator S ($\langle JS\rangle$, $\langle QS\rangle$, $\langle SS\rangle$) diverge when β goes to zero at small ω. We have confirmed that (4.65)–(4.70) agree to the numerical results in figure 6, 12 and 13.

If we define a normal fluid density (K_n) as

$$K_n \equiv \frac{\beta}{\mu} \lim_{\omega\to 0} \frac{\mathrm{Im}[\langle JS\rangle]}{\omega}\,, \tag{4.72}$$

the Ward identity (4.61) yields the charge conservation $n = \mu K_s + \mu K_n$. In figure 8, we plot n/μ^2(dotted curves) and K_s/μ(solid curves) versus T/T_c at several μ/βs. The difference between the dotted and solid curve at a given μ/β is K_n/μ. As temperature approaches to zero,[14] K_n vanishes for $\mu/\beta \gtrsim 2$ (figure 8(b)) while K_n is nonzero for $\mu/\beta \lesssim 2$ (figure 8(a)). Interestingly, it seems that this transition conicide with the coherent/incoherent metal transition studied in [31], where the metal state of this model was classified as coherent state with a well defined Drude peak in AC conductivity for $\mu/\beta \lesssim 2$ and incoherent state without a Drude peak for $\mu/\beta \lesssim 2$.[15] In coherent state, the normal fluid density K_n can be used as an input parameter to fit the Drude formula in the two fluid model of holographic superconductors [42]. The non-zero K_n at zero temperature for large momentum relaxation has been also observed in a holographic superconductor dual to a helical lattice [47].

5 Homes' law and Uemura's law

Homes' law (1.1) and Uemura's law (1.2) were introduced in section 1. In this section we check if Homes' law and Uemura's law are realized in our model (2.1) with nonzero q. For $q = 0$ the system is not a holographic superconductor as shown in section 3. The scalar

[14] Our numerics becomes unstable near zero temperature, so we present data up to the lowest possible temperature in our numerics.

[15] Here, the metal state means both normal phase and the normal component of the two fluid model in superconductor phase.

JHEP10(2016)041

ψ_I giving momentum relaxation is essential for Homes' law because without momentum relaxation $\sigma_{\rm DC}$ is infinite and Homes' law cannot be satisified.

Homes' law and Uemura's law are material independent universal scaling relations observed in high temperature superconductor as well as conventional superconductors [47, 56–58]. Uemura's law appearing in underdoped cuprates is

$$\tilde{\rho}_s(\tilde{T}=0) = B\,\tilde{T}_c\,, \tag{5.1}$$

and Homes' law satisfied in a broader class of materials is

$$\tilde{\rho}_s(\tilde{T}=0) = C\sigma_{\rm DC}(\tilde{T}_c)\,\tilde{T}_c\,, \tag{5.2}$$

where B and C are material independent universal constants. Here, the superfluid density ($\tilde{\rho}_s$), temperature($\tilde{T}$), and conductivity($\sigma_{\rm DC}$) are all dimensionless [47]. In this subsection we use momentum relaxation strength parameter(β) as our scale so we choose $\tilde{\rho}_s = K_s/\beta$ and $\tilde{T} = T/\beta$. In our model, there are two free parameters, μ/β and q. Thus universality of B and C means that B and C are independent of μ/β and q. To check this it is convenient to fix q first, and make plots of B and C vs μ/β for Uemura's law and Homes' law respectively.

To compute B and C,

$$B = \frac{\tilde{\rho}_s}{\tilde{T}_c} = \frac{K_s}{T_c}\,, \qquad C = \frac{\tilde{\rho}_s}{\sigma_{\rm DC}\tilde{T}_c} = \frac{K_s}{\sigma_{\rm DC}T_c}\,, \tag{5.3}$$

the superfluid density $\tilde{\rho}_s(=\mu/\beta\cdot K_s/\mu)$ can be read off from the solid curves in figure 8, where the curves do not reach to $T=0$ because of instability of numerical analysis. Therefore, we extrapolated the curves up to zero temperature to read $\tilde{\rho}_s$ at $T=0$. The conductivity $\sigma_{\rm DC}$ can be read in figure 2 or analytically $\sigma_{\rm DC} = 1+\mu^2/\beta^2$ in our model [28]. The transition temperature $\tilde{T}_c$ has been computed numerically in [46]. Our numerical results of $\tilde{\rho}_s, \tilde{T}_c$ and $\sigma_D C$ for $q=3$ are shown in figure 9.

From figure 9 we may expect that there is a linear relation between $\tilde{\rho}_s$ and $\tilde{T}_c$ at least for large μ/β, which supports Uemura's law. To see if this is the case also for small μ/β we make a plot of B vs μ/β in figure 10(a), where we find that Uemura's law holds only for $\mu/\beta \gtrsim 2$, of which data are red dots. Interestingly, the parameter regime $\mu/\beta \gtrsim 2$ (red dots) belongs to coherent metal regime, where the optical conductivity of normal component shows a Drude peak behaviour. Furthermore, this regime corresponds to figure 8(b), where charge density is the same as superfluid density at zero temperature. The blue dots belong to incoherent regime, where a optical conductivity loses a Drude behaviour. They correspond to figure 8(a) and there is a gap between charge density and superfluid density at zero temperature. Also, for different values of q, we find that Uemura's law is satisfied for large μ/β but with a different constant B. For example, for $q=2$, $B\approx 6.87$ and for $q=6$, $B\approx 4.64$ in the regime of $\mu/\beta \gtrsim 2$ (figure 10(c)). Since Uemura's law is observed in underdoped regimes, if β can be interpreted as a doping parameter our result will be consistent with phenomena.

JHEP10(2016)041

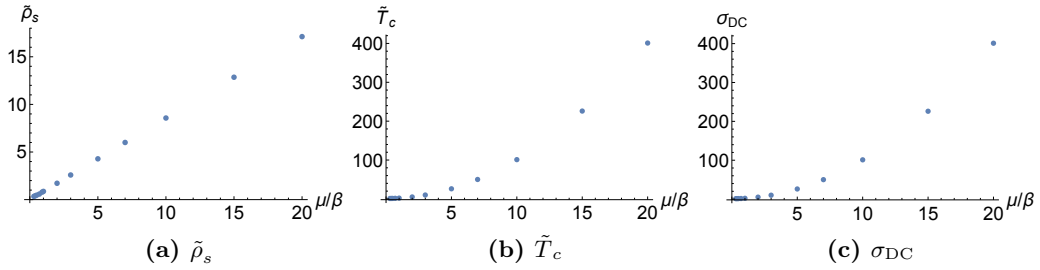

(a) $\tilde{\rho}_s$ **(b)** $\tilde{T}_c$ **(c)** $\sigma_{\rm DC}$

Figure 9. $\tilde{\rho}_s, \tilde{T}_s$, and $\sigma_{\rm DC}$ for $q = 3$.

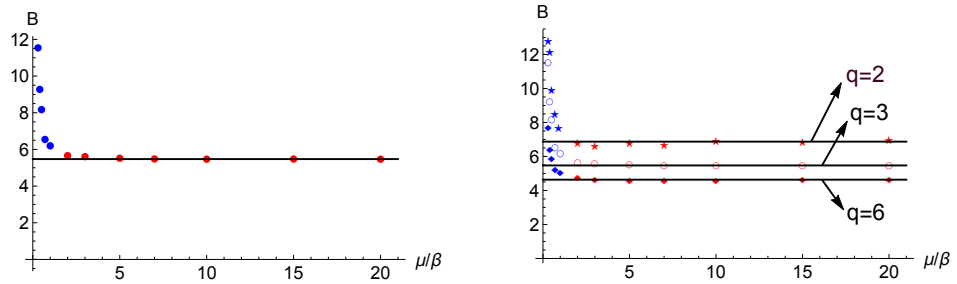

(a) $B(=\tilde{\rho}_s/\tilde{T}_c)$, $q = 3$ **(b)** $B(=\tilde{\rho}_s/\tilde{T}_c)$ for $q = 2, 3, 6$

Figure 10. Checking Uemura's law. Uemura's law holds in coherent regime (red dots: $\mu/\beta = 2, 3, 5, 7, 10, 15, 20$) while it does not hold in incoherent regime (blue dots: $\mu/\beta = 0.3, 0.4, 0.5, 0.7, 1$). In (a) the black line is drawn for $B \sim 5.47$, and in (b) the black lines are drawn for $B \sim 6.87, 5.47, 4.64$ for $q = 2, 3, 6$ respectively.

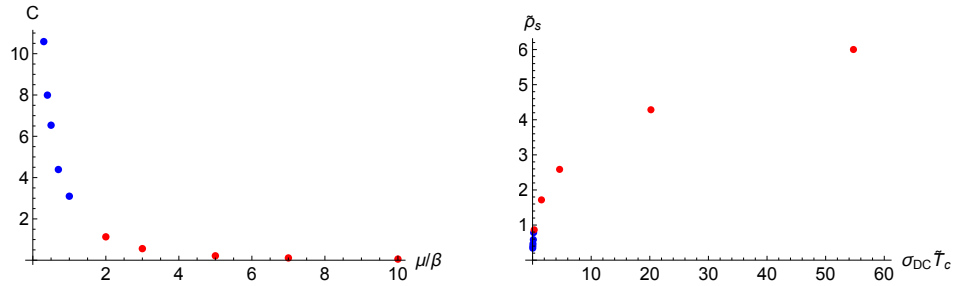

(a) $C(=\tilde{\rho}_s/(\sigma_{\rm DC}\tilde{T}_c))$, $q = 3$ **(b)** $\tilde{\rho}_s$ vs $\sigma_{\rm DC}\tilde{T}_c$, $q = 3$

Figure 11. Checking Homes' law. Homes' law does not hold. The blue dots are for incoherent regime ($\mu/\beta = 0.3, 0.4, 0.5, 0.7, 1$) and the red dots are for coherent regime ($\mu/\beta = 2, 3, 5, 7, 10$). In (a) the data for C do not align on a constant value and in (b) the data do not yield a linear relation.

Based on our results on Uemura's law (figure 10(a)) and $\sigma_{\rm DC}$ (figure 9(c)), we may anticipate if Homes' law is satisfied. If $\sigma_{\rm DC}$ is quickly decreasing function approaching to constant for $\mu/\beta \gtrsim 2$ we may have a chance to obtain Homes' law. However, our $\sigma_{\rm DC}$ does not show that behaviour. Therefore, as shown in figure 11, Home's law does not hold in both coherent regime (red dots) and incoherent regime (blue dots). In figure 11(a), for

JHEP10(2016)041

large μ/β, $C(=\tilde{\rho}_s/(\sigma_{\rm DC}\tilde{T}_c))$ approaches to a constant value, but it is zero. It simply means that $\sigma_{\rm DC}$ goes to infinite as momentum relaxation goes to zero. Figure 11(b) is another representation, a plot of $\tilde{\rho}_s$ versus $\sigma_{\rm DC}\tilde{T}_c$, where it is also clear that there is no linear relation between between $\tilde{\rho}_s$ and $\sigma_{\rm DC}\tilde{T}_c$. For different values of q, we considered $q = 2$ and $q = 6$ and obtained figures qualitatively similar to figure 11, so Homes' law seems not satisfied for different values of q either.

Homes' law may be understood based on Planckian dissipation, for which the time scale of dissipation is shortest possible [60]. In summary, the left hand side of (5.2), superfluid density is proportional to density of mobile electrons in superconducting state (n_S). The right hand side of (5.2), $\sigma_{\rm DC}$ is proportional to density of mobile electrons in normal state (n_N) times relaxation time (τ), and the relaxation time is inversely proportional to the temperature (Planckian dissipation):

$$\rho_s \sim n_S\,, \qquad \sigma_{\rm DC} \sim n_N \tau(T_c)\,, \qquad \tau(T_c) \approx \frac{\hbar}{k_B T_c}\,, \tag{5.4}$$

where k_B is Boltzmann's constant and proportionality constants of the relations are material independent. Notice that thanks to the Planckian dissipation T_c is cancelled out in Homes' law, leaving universal constant $\hbar/k_B$. Finally if we use another empirical law, Tanner's law, $n_S = n_N/4$, Homes' law is obtained.

In our model, it turns out a kind of Tanner's law holds in coherent metal regime ($\mu/\beta \geq 2$), where momentum relaxation is weak. In figure 8(b), all curves coincide and it means n_s/n_N does not depend on μ/β, which is the qualitative content of Tanner's law. Therefore, if our system were Planckian dissipator in coherent regime, we would have seen Homes' law. The relaxation time τ for our model can be written as

$$\tau = \frac{f(T/\beta, \mu/\beta, q)}{T}\,, \tag{5.5}$$

where T in the denominator is extracted to mimic the form of Planckian dissipation [47]. Since our system does not show Homes' law it is not a Planckian dissipator, which means f is not universal near T_c. Furthermore, we may induce that $f \sim \mu^2/\beta^2$ because $T_c \sim \mu/\beta$ from figure 9(b) and $\tau \sim \mu/\beta$ from the analysis in [31]. Indeed, it was shown that in general the system could not be a Planckian dissipator if momentum is relaxed weakly [47].

Our results on Uemura's law and Homes' law are different from the previous work [47], where a superconductor model in a helical lattice was studied. In the model, there are two parameters corresponding to the strength of momentum relaxation effect: the lattice strength λ and the helix pitch p, and it was found that Homes' law held for restricted parameter regime (not in small momentum relaxation, but for rather large values of λ and p) while Uemura's law did not hold. In particular, Homes' law was observed in insulating phase near phase transition. However, in our model there is no insulating phase and it may be a reason why two models show different results. There are other differences between two models. The model in helix lattice is anisotropic five dimensional model, while our model is isotropic four dimensional.

JHEP10(2016)041

6 Conclusion and discussions

In this paper, we analysed a holographic superconductor model incorporating momentum relaxation. Building on previous works [31, 46, 53, 54], we focused on three issues, where momentum relaxation plays an important role. (1) Ward identities: constraints between conductivities, (2) conductivities with a neutral scalar hair instability, (3) Homes' law and Uemura's law.

In holographic methods, we often need to solve complicated differential equations which do not allow analytic solutions, so it is important to develop reliable and systematic numerical methods. Computing AC conductivities is such an example, for which we have developed a numerical method. However, to make sure our numerics are reliable and robust, it will be good to have a cross-check. The Ward identity serves as a nice cross-check of our numerical method since we can compare our numerical results with the independently derived analytic formula. When there is a neutral scalar instability we explicitly showed that the DC electric conductivity is finite, while it is infinite for a complex scalar instability. This shows that the neutral scalar instability has nothing to do with superconductivity as expected.

Homes' law is very interesting and important not only because of its material independent universality but also a possible relation to quantum criticality and Planckian dissipation, which also underpins the universal bound of the viscosity to entropy in strongly correlated systems such as quark-gluon plasma. We have checked Homes' law and Uemura's law in our model. It turns out that Homes' law does not hold and Umeura's law holds for small momentum relaxation related to coherent metal regime. Our results are different from [47], where a holographic superconductor in a helical lattice was considered and it was shown that Homes' law is satisfied for some restricted parameter regime in insulating phase, while Uemuras' law is not satisfied at all. The difference may be due to the existence of insulating phase and/or anisotropy in a model with a helical lattice. To clarify it, it will be helpful to study Homes' law in different holographic superconductor models such as anisotropic massless scalar model, Q-lattice model, or massive gravity model [68].

Regarding Homes' law and Uemura's law, there may be an issue in the identification of the superfulid density. We have found that superfluid density and total charge density at zero temperature do not agree at large momentum relaxation, similarly to the case in a helical lattice [47]. Because the Ferrell-Glover-Tinkham (FGT) sum rule still holds in our model [46], it is possible that part of the low frequency spectral weight are transferred to intermediate frequencies instead of the superfluid pole. Therefore, as a cross check, it will be good to compute the superfluid density from the transverse response by the magnetic/London penetration depth, for which we need to solve for the transverse propagator at small non-zero momentum [47]. There is also another closely related quantity to superfluid density. By integrating a Maxwell's equation over the holographic coordinate r,

$$\nabla_M F^{tM} = iq\left(\Phi^* D^t\Phi - \Phi D^t\Phi^*\right), \tag{6.1}$$

we may define the charge density of hair outside the horizon, n_{hair}, as

$$n_{\text{hair}} \equiv n - n_h \equiv \sqrt{-g}F^{tr}|_{r=\infty} - \sqrt{-g}F^{tr}|_{r=r_h} = iq\int_{r_h}^{\infty} dr\sqrt{-g}\left(\Phi^* D^t\Phi - \Phi D^t\Phi^*\right), \tag{6.2}$$

JHEP10(2016)041

where n is the charge density of the dual field theory and n_h is interpreted as the charge density inside the horizon. In normal phase $n_{\text{hair}} = 0$ while in superconducting phase $n_{\text{hair}} \neq 0$. Therefore, n_{hair} plays a role of order parameter of superconducting phase transition. For $q = 0$, n_{hair} is zero so K_s is zero, which is consistent with our results in section 3. However, it turns out that the numerical value of K_s is different from n_{hair}. We have checked Homes' law and Uemura's law by using n_{hair} as the superfulid density, but it did not support Homes' law and Uemura's law. It will be interesting to find a physical meaning of n_{hair} in the dual field theory and the precise relation to superfluid density.

Acknowledgments

We would like to thank Johanna Erdmenger, Steffen Klug, Rene Meyer, Yunseok Seo, Sang-Jin Sin for valuable discussions and correspondence. The work of K.Y.Kim and K.K.Kim was supported by Basic Science Research Program through the National Research Foundation of Korea(NRF) funded by the Ministry of Science, ICT & Future Planning(NRF-2014R1A1A1003220) and the GIST Research Institute(GRI) in 2016. K.K.Kim was also supported by the National Research Foundation of Korea(NRF) grant with the grant number NRF-2015R1D1A1A 01058220. M. Park is supported by TJ Park Science Fellowship of POSCO TJ Park Foundation.

A Two-point functions related to the real scalar operator

As commented at the end of section 4, we have confirmed the Ward identities numerically for other cases too: 1) $B = 0, \beta/\mu = 0.1$, 2) $B = 0, \mu = 0$, 3) $B \neq 0$. For completeness, we show here the numerical data of $\langle JS \rangle$, $\langle QS \rangle$, $\langle SS \rangle$ for (1) and (2) in figure 12 and 13 respectively. For electric, thermoelectric and thermal conductivities we refer to [31, 54]. In figure 14 we show the numerical results of Ward identites for (3).

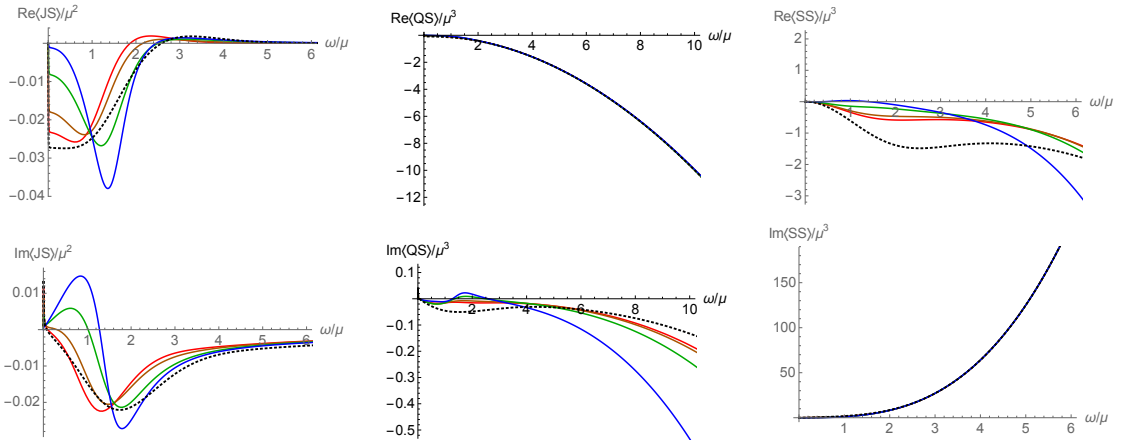

Figure 12. $\langle JS \rangle$, $\langle QS \rangle$, $\langle SS \rangle$ for $\beta/\mu = 0.1$. $T/T_c = 1.5, 1, 0.94, 0.76, 0.37$ (dotted, red, orange, green, blue).

JHEP10(2016)041

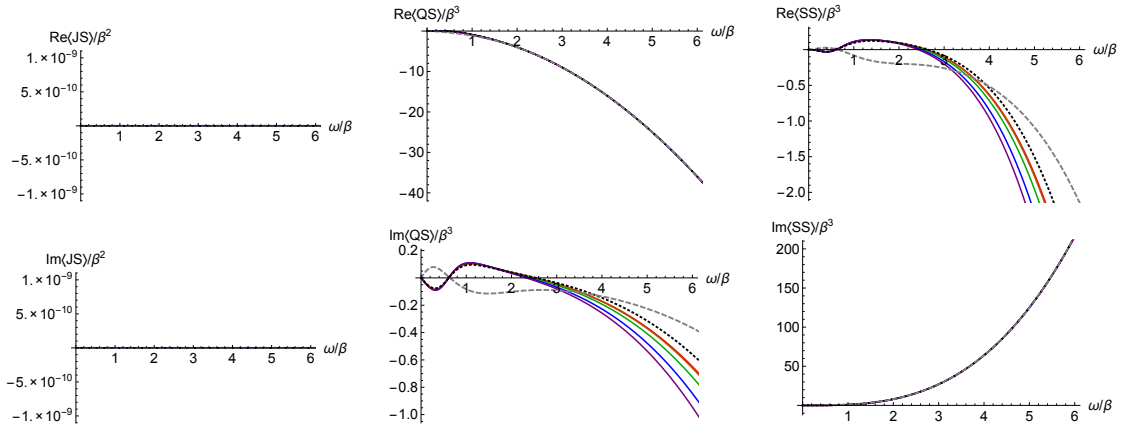

Figure 13. $\langle JS\rangle$, $\langle QS\rangle$, $\langle SS\rangle$ for $\mu = 0$. $T/T_c = 13.2, 3.5, 1, 0.95, 0.7, 0.4, 0.25$ (dashed, dotted, red, orange, green, blue, purple).

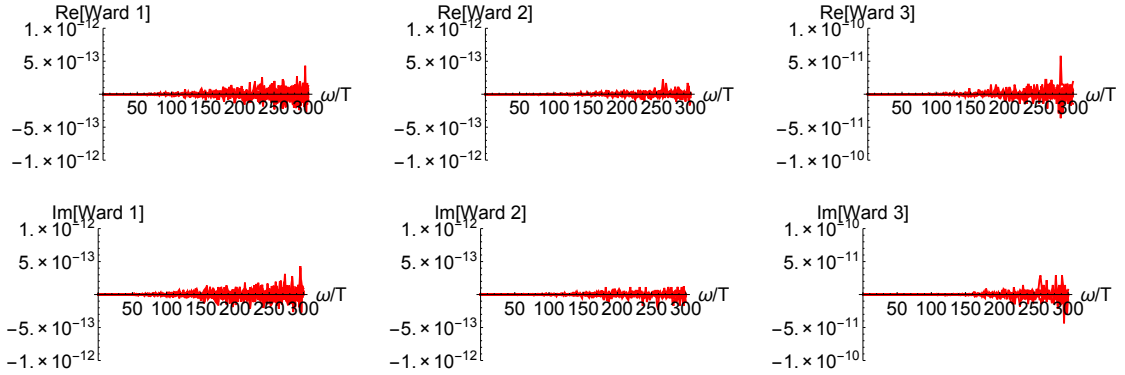

(a) Ward 1: (4.44) **(b)** Ward 2: (4.45) **(c)** Ward 3: (4.46)

Figure 14. Finite B filed case: we plotted all components of the Ward identities (4.44)–(4.46) together for the case with $\mu/T = 1$, $B/T = 3$ and $\beta/\mu = 0, 0.5, 1, 1.5$.

References

[1] J. Casalderrey-Solana, H. Liu, D. Mateos, K. Rajagopal and U.A. Wiedemann, *Gauge/String Duality, Hot QCD and Heavy Ion Collisions*, arXiv:1101.0618 [INSPIRE].

[2] S.A. Hartnoll, *Lectures on holographic methods for condensed matter physics*, *Class. Quant. Grav.* **26** (2009) 224002 [arXiv:0903.3246] [INSPIRE].

[3] C.P. Herzog, *Lectures on Holographic Superfluidity and Superconductivity*, *J. Phys.* **A 42** (2009) 343001 [arXiv:0904.1975] [INSPIRE].

[4] N. Iqbal, H. Liu and M. Mezei, *Lectures on holographic non-Fermi liquids and quantum phase transitions*, arXiv:1110.3814 [INSPIRE].

JHEP10(2016)041

[5] J. Zaanen, Y.-W. Sun, Y. Liu and K. Schalm, *Holographic Duality in Condensed Matter Physics*, Cambridge University Press, Cambridge, U.K. (2015).

[6] M. Ammon and J. Erdmenger, *Gauge/gravity duality*, Cambridge University Press, Cambridge, U.K. (2015).

[7] S.A. Hartnoll, C.P. Herzog and G.T. Horowitz, *Building a Holographic Superconductor*, *Phys. Rev. Lett.* **101** (2008) 031601 [arXiv:0803.3295] [INSPIRE].

[8] S.A. Hartnoll, C.P. Herzog and G.T. Horowitz, *Holographic Superconductors*, *JHEP* **12** (2008) 015 [arXiv:0810.1563] [INSPIRE].

[9] G.T. Horowitz, *Introduction to Holographic Superconductors*, *Lect. Notes Phys.* **828** (2011) 313 [arXiv:1002.1722] [INSPIRE].

[10] R.-G. Cai, L. Li, L.-F. Li and R.-Q. Yang, *Introduction to Holographic Superconductor Models*, *Sci. China Phys. Mech. Astron.* **58** (2015) 060401 [arXiv:1502.00437] [INSPIRE].

[11] G.T. Horowitz, J.E. Santos and D. Tong, *Optical Conductivity with Holographic Lattices*, *JHEP* **07** (2012) 168 [arXiv:1204.0519] [INSPIRE].

[12] G.T. Horowitz, J.E. Santos and D. Tong, *Further Evidence for Lattice-Induced Scaling*, *JHEP* **11** (2012) 102 [arXiv:1209.1098] [INSPIRE].

[13] Y. Ling, C. Niu, J.-P. Wu and Z.-Y. Xian, *Holographic Lattice in Einstein-Maxwell-Dilaton Gravity*, *JHEP* **11** (2013) 006 [arXiv:1309.4580] [INSPIRE].

[14] P. Chesler, A. Lucas and S. Sachdev, *Conformal field theories in a periodic potential: results from holography and field theory*, *Phys. Rev.* **D 89** (2014) 026005 [arXiv:1308.0329] [INSPIRE].

[15] A. Donos and J.P. Gauntlett, *The thermoelectric properties of inhomogeneous holographic lattices*, *JHEP* **01** (2015) 035 [arXiv:1409.6875] [INSPIRE].

[16] D. Vegh, *Holography without translational symmetry*, arXiv:1301.0537 [INSPIRE].

[17] R.A. Davison, *Momentum relaxation in holographic massive gravity*, *Phys. Rev.* **D 88** (2013) 086003 [arXiv:1306.5792] [INSPIRE].

[18] M. Blake and D. Tong, *Universal Resistivity from Holographic Massive Gravity*, *Phys. Rev.* **D 88** (2013) 106004 [arXiv:1308.4970] [INSPIRE].

[19] M. Blake, D. Tong and D. Vegh, *Holographic Lattices Give the Graviton an Effective Mass*, *Phys. Rev. Lett.* **112** (2014) 071602 [arXiv:1310.3832] [INSPIRE].

[20] A. Amoretti, A. Braggio, N. Maggiore, N. Magnoli and D. Musso, *Thermo-electric transport in gauge/gravity models with momentum dissipation*, *JHEP* **09** (2014) 160 [arXiv:1406.4134] [INSPIRE].

[21] A. Amoretti, A. Braggio, N. Maggiore, N. Magnoli and D. Musso, *Analytic dc thermoelectric conductivities in holography with massive gravitons*, *Phys. Rev.* **D 91** (2015) 025002 [arXiv:1407.0306] [INSPIRE].

[22] A. Amoretti and D. Musso, *Magneto-transport from momentum dissipating holography*, *JHEP* **09** (2015) 094 [arXiv:1502.02631] [INSPIRE].

[23] A. Donos and J.P. Gauntlett, *Holographic Q-lattices*, *JHEP* **04** (2014) 040 [arXiv:1311.3292] [INSPIRE].

JHEP10(2016)041

[24] A. Donos and J.P. Gauntlett, *Novel metals and insulators from holography*, *JHEP* **06** (2014) 007 [arXiv:1401.5077] [INSPIRE].

[25] Y. Ling, P. Liu, C. Niu, J.-P. Wu and Z.-Y. Xian, *Holographic fermionic system with dipole coupling on Q-lattice*, *JHEP* **12** (2014) 149 [arXiv:1410.7323] [INSPIRE].

[26] Y. Ling, P. Liu and J.-P. Wu, *A novel insulator by holographic Q-lattices*, *JHEP* **02** (2016) 075 [arXiv:1510.05456] [INSPIRE].

[27] Y. Ling, P. Liu, C. Niu and J.-P. Wu, *Pseudo-gap phase and duality in a holographic fermionic system with dipole coupling on Q-lattice*, *Chin. Phys.* **C 40** (2016) 043102 [arXiv:1602.06062] [INSPIRE].

[28] T. Andrade and B. Withers, *A simple holographic model of momentum relaxation*, *JHEP* **05** (2014) 101 [arXiv:1311.5157] [INSPIRE].

[29] B. Goutéraux, *Charge transport in holography with momentum dissipation*, *JHEP* **04** (2014) 181 [arXiv:1401.5436] [INSPIRE].

[30] M. Taylor and W. Woodhead, *Inhomogeneity simplified*, *Eur. Phys. J.* **C 74** (2014) 3176 [arXiv:1406.4870] [INSPIRE].

[31] K.-Y. Kim, K.K. Kim, Y. Seo and S.-J. Sin, *Coherent/incoherent metal transition in a holographic model*, *JHEP* **12** (2014) 170 [arXiv:1409.8346] [INSPIRE].

[32] Y. Bardoux, M.M. Caldarelli and C. Charmousis, *Shaping black holes with free fields*, *JHEP* **05** (2012) 054 [arXiv:1202.4458] [INSPIRE].

[33] N. Iizuka and K. Maeda, *Study of Anisotropic Black Branes in Asymptotically anti-de Sitter*, *JHEP* **07** (2012) 129 [arXiv:1204.3008] [INSPIRE].

[34] L. Cheng, X.-H. Ge and S.-J. Sin, *Anisotropic plasma at finite* U(1) *chemical potential*, *JHEP* **07** (2014) 083 [arXiv:1404.5027] [INSPIRE].

[35] L.-Q. Fang, X.-M. Kuang, B. Wang and J.-P. Wu, *Fermionic phase transition induced by the effective impurity in holography*, *JHEP* **11** (2015) 134 [arXiv:1507.03121] [INSPIRE].

[36] Y. Seo, K.-Y. Kim, K.K. Kim and S.-J. Sin, *Character of matter in holography: Spin-orbit interaction*, *Phys. Lett.* **B 759** (2016) 104 [arXiv:1512.08916] [INSPIRE].

[37] T. Andrade and A. Krikun, *Commensurability effects in holographic homogeneous lattices*, *JHEP* **05** (2016) 039 [arXiv:1512.02465] [INSPIRE].

[38] T. Andrade, *A simple model of momentum relaxation in Lifshitz holography*, arXiv:1602.00556 [INSPIRE].

[39] A. Donos and S.A. Hartnoll, *Interaction-driven localization in holography*, *Nature Phys.* **9** (2013) 649 [arXiv:1212.2998] [INSPIRE].

[40] A. Donos, B. Goutéraux and E. Kiritsis, *Holographic Metals and Insulators with Helical Symmetry*, *JHEP* **09** (2014) 038 [arXiv:1406.6351] [INSPIRE].

[41] A. Donos, J.P. Gauntlett and C. Pantelidou, *Conformal field theories in $d = 4$ with a helical twist*, *Phys. Rev.* **D 91** (2015) 066003 [arXiv:1412.3446] [INSPIRE].

[42] G.T. Horowitz and J.E. Santos, *General Relativity and the Cuprates*, *JHEP* **06** (2013) 087 [arXiv:1302.6586] [INSPIRE].

[43] H.B. Zeng and J.-P. Wu, *Holographic superconductors from the massive gravity*, *Phys. Rev.* **D 90** (2014) 046001 [arXiv:1404.5321] [INSPIRE].

JHEP10(2016)041

[44] Y. Ling, P. Liu, C. Niu, J.-P. Wu and Z.-Y. Xian, *Holographic Superconductor on Q-lattice*, *JHEP* **02** (2015) 059 [arXiv:1410.6761] [INSPIRE].

[45] T. Andrade and S.A. Gentle, *Relaxed superconductors*, *JHEP* **06** (2015) 140 [arXiv:1412.6521] [INSPIRE].

[46] K.-Y. Kim, K.K. Kim and M. Park, *A Simple Holographic Superconductor with Momentum Relaxation*, *JHEP* **04** (2015) 152 [arXiv:1501.00446] [INSPIRE].

[47] J. Erdmenger, B. Herwerth, S. Klug, R. Meyer and K. Schalm, *S-Wave Superconductivity in Anisotropic Holographic Insulators*, *JHEP* **05** (2015) 094 [arXiv:1501.07615] [INSPIRE].

[48] M. Baggioli and M. Goykhman, *Phases of holographic superconductors with broken translational symmetry*, *JHEP* **07** (2015) 035 [arXiv:1504.05561] [INSPIRE].

[49] M. Baggioli and M. Goykhman, *Under The Dome: Doped holographic superconductors with broken translational symmetry*, *JHEP* **01** (2016) 011 [arXiv:1510.06363] [INSPIRE].

[50] J.-i. Koga, K. Maeda and K. Tomoda, *Holographic superconductor model in a spatially anisotropic background*, *Phys. Rev.* **D 89** (2014) 104024 [arXiv:1401.6501] [INSPIRE].

[51] X. Bai, B.-H. Lee, M. Park and K. Sunly, *Dynamical Condensation in a Holographic Superconductor Model with Anisotropy*, *JHEP* **09** (2014) 054 [arXiv:1405.1806] [INSPIRE].

[52] A. Donos and J.P. Gauntlett, *Thermoelectric DC conductivities from black hole horizons*, *JHEP* **11** (2014) 081 [arXiv:1406.4742] [INSPIRE].

[53] K.-Y. Kim, K.K. Kim, Y. Seo and S.-J. Sin, *Gauge Invariance and Holographic Renormalization*, *Phys. Lett.* **B 749** (2015) 108 [arXiv:1502.02100] [INSPIRE].

[54] K.-Y. Kim, K.K. Kim, Y. Seo and S.-J. Sin, *Thermoelectric Conductivities at Finite Magnetic Field and the Nernst Effect*, *JHEP* **07** (2015) 027 [arXiv:1502.05386] [INSPIRE].

[55] S.A. Hartnoll and C.P. Herzog, *Ohm's Law at strong coupling: S duality and the cyclotron resonance*, *Phys. Rev.* **D 76** (2007) 106012 [arXiv:0706.3228] [INSPIRE].

[56] C.C. Homes, S.V. Dordevic, T. Valla and M. Strongin, *Scaling of the superfluid density in high-temperature superconductors*, *Phys. Rev.* **B 72** (2005) 134517 [cond-mat/0410719].

[57] C.C. Homes et al., *Universal scaling relation in high-temperature superconductors*, *Nature* **430** (2004) 539 [cond-mat/0404216] [INSPIRE].

[58] J. Erdmenger, P. Kerner and S. Muller, *Towards a Holographic Realization of Homes' Law*, *JHEP* **10** (2012) 021 [arXiv:1206.5305] [INSPIRE].

[59] S. Sachdev and B. Keimer, *Quantum Criticality*, *Phys. Today* **64N2** (2011) 29 [arXiv:1102.4628] [INSPIRE].

[60] J. Zaanen, *Superconductivity: Why the temperature is high*, *Nature* **430** (2004) 512.

[61] M. Bianchi, D.Z. Freedman and K. Skenderis, *Holographic renormalization*, *Nucl. Phys.* **B 631** (2002) 159 [hep-th/0112119] [INSPIRE].

[62] S.A. Hartnoll and P. Kovtun, *Hall conductivity from dyonic black holes*, *Phys. Rev.* **D 76** (2007) 066001 [arXiv:0704.1160] [INSPIRE].

[63] T. Albash and C.V. Johnson, *Vortex and Droplet Engineering in Holographic Superconductors*, *Phys. Rev.* **D 80** (2009) 126009 [arXiv:0906.1795] [INSPIRE].

[64] K. Maeda, M. Natsuume and T. Okamura, *Vortex lattice for a holographic superconductor*, *Phys. Rev.* **D 81** (2010) 026002 [arXiv:0910.4475] [INSPIRE].

JHEP10(2016)041

[65] D.T. Son and A.O. Starinets, *Minkowski space correlators in AdS/CFT correspondence: Recipe and applications*, *JHEP* **09** (2002) 042 [hep-th/0205051] [INSPIRE].

[66] J. Lindgren, I. Papadimitriou, A. Taliotis and J. Vanhoof, *Holographic Hall conductivities from dyonic backgrounds*, *JHEP* **07** (2015) 094 [arXiv:1505.04131] [INSPIRE].

[67] C.P. Herzog, N. Lisker, P. Surowka and A. Yarom, *Transport in holographic superfluids*, *JHEP* **08** (2011) 052 [arXiv:1101.3330] [INSPIRE].

[68] K.-Y. Kim and C. Niu, *Homes' law in Holographic Superconductor with Q-lattices*, arXiv:1608.04653 [INSPIRE].

JHEP10(2016)041